MINERALISED PHYTOPLANKTON COMMUNITY COMPOSITION IN THE SCOTIA AND WEDDELL SEAS (SOUTHERN OCEAN), WITH EMPHASIS ON DIATOMS AND COCCOLITHOPHORES

Amy Harington

Thesis presented in 2012 in fufillment of the requirements for the degree Master of Science in Zoology

Supervisors

Mike Lucas (University of Cape Town - Cape Town, South Africa)

Alex Poulton (National Oceanographic Centre - Southampton, United Kingdom)

Plagiarism Declaration

1. I know that plagiarism is wrong. Plagiarism is to use another's work and pretend that it is one's own.
2. I have used the Harvard System of Referencing for citation and referencing. Each contribution to, and quotation in, this thesis from the work(s) of other people has been attributed, and has been cited and referenced.
3. This thesis is my own work.
4. I have not allowed, and will not allow, anyone to copy my work with the intention of passing it off as his or her own work.

Signature _____

Abstract

Phytoplankton community composition in the Southern Ocean (SO) determines levels of primary production, which support marine ecosystems and export of material to the deep sea. Nanoplankton (cell diameters 2-20 μm) are poorly resolved by traditional microscopy, and it is becoming apparent that unknown diversity and ecosystem functionality may be contained in this size class: for example, small diatoms (<10 μm) appear widespread in the SO, and may limit our understanding of the response of phytoplankton communities to climate change. In order to address these issues we analysed water samples using Scanning Electron Microscopy from a transect between Antarctica and South Georgia, as part of the 2008-2009 South African National Antarctic Expedition. Multivariate analysis distinguished two distinct communities: one in the Weddell Sea and the other in the east Scotia Sea. The coccolithophorid *Emiliania huxleyi* and the chrysophyte *Tetraparma pelagica* were common in the east Scotia Sea, although the Ligeti Ridge (60°S) acted as the southernmost boundary for *E. huxleyi*. A statistical comparison of community composition and environmental data showed that silicic acid concentration and sea surface temperature were the major factors driving phytoplankton species distribution. Cell counts also indicated that the nanoplankton size class represented a substantial fraction (57-97%) of the total community abundance, which implies that traditional phytoplankton methods may have underestimated the importance of small mineralising nanoplankton. However, with respect to cell carbon, the smaller size class 0–99 pg C cell^{-1} represents between 0 and 60% of the total community biomass. Underestimation of the biomass of this important algal group, and its role in primary production and export, may inhibit our understanding of how plankton communities may respond to climate change.

Contents

List of Figures

List of Tables

List of Acronyms

ACC – Antarctic Circumpolar Current

APF – Antarctic Polar Front

CTD – Conductivity Temperature Depth

HNLC – High Nutrient Low Chlorophyll

MDS – Multi-Dimensional Scaling

MIZ – Marginal Ice Zone

MLD – Mixed Layer Depth

PC – Principle Component

PCA – Principle Component Analysis

PF – Polar Front

PGT – Princeton Gamma Technology

PRIMER – Plymouth Routines In Multivariate Ecological Research

SACCB – Southern Antarctic Circumpolar Boundary

SACCF – Southern Antarctic Circumpolar Front

SAF – Subantarctic Front

SANAE – South African National Antarctic Expedition

Acknowledgements

I should like to express my sincere gratitude to my thesis supervisors, Dr Mike Lucas and Dr Alex Poulton. Their constant encouragement, advice and mentorship have been invaluable throughout this project. I would also like to thank the SANAE 49 oceanographic team; Dr Sandy Thomalla, Dr Yuri Cotroneo, Dr Thabo Mtshali, Dr Robert Scholes Ceinwen Smith, Sarah Nicholson, Fiona Preston-Whyte, Samantha Ehrlich, and Patrick Hayes-Foley without whom there would be no data for this thesis and the long months at sea would have been unbearable. Specifically, Dr Thomalla for her endless advice and encouragement, Seb Swart for his advice on mixed layer depths and Nicolas Fauchereau for his help with sea ice.

I would like to further thank, the South African National Antarctic Program (SANAP) and the captain and crew of the SA Agulhas. The National Research Foundation provided financial support.

A final thank you to my wonderful family for all their support.

1 Introduction

1.1 The Southern Ocean

The Southern Ocean is defined as the oceanic area south of ~40°S (Sullivan et al., 1993), and covers a surface area exceeding 20 million km^2. The Southern Ocean also has the greatest stock of unused macronutrients (Levitus et al., 1993), which are available at high concentrations (NO_3^-, ~25 µm to 30 µm; $Si(OH)_4$, 20 µm to 60 µm). It is one of the few oceanic provinces where these macronutrients are significantly underutilized (Arrigo et al., 1998) and total biological primary and export production are far below their potential level (Falkowski, 1998). The Southern Ocean is a High Nutrient Low Chlorophyll (HNLC) region and is the largest one in the world (Martin, 1990), with a high potential effect on atmospheric CO_2 concentrations (Falkowski, 1998). However, certain areas of the Southern Ocean exhibit high chlorophyll (chl-*a*) and phytoplankton biomass (Boyd, 2002), and these 'hot spots' are sustained by natural iron fertilization (e.g., Blain et al., 2007; Pollard et al., 2009; Hinz et al. 2012). High chl-*a* biomass is observed in the marginal ice zone (MIZ), where the retreating ice edge supplies dissolved iron, while adding mixed layer stability through ice-melt. Such ice-melt also provides algal seed stocks (Sedwick and Ditullio, 1997; Wright and van den Enden, 2000; Grotti et al., 2005; Gomi et al., 2007; Lannuzel et al., 2007; Wright et al., 2010). Frontal regions associated with mesoscale physical processes lead to increased productivity (de Baar et al., 1995; Laubscher et al., 1993; Moore et al., 1999; Moore and Abbott, 2002; Sokolov and Rintoul, 2002).

Despite very patchy phytoplankton biomass and productivity, the Southern Ocean is considered a major sink for anthropogenic CO_2 (Sabine et al., 2004; Arrigo et al., 2008; Gruber et al., 2009; Takahashi et al., 2009), presently taking up a third of all anthropogenic CO_2 despite only representing ~20% of the global ocean by surface area (Gruber et al., 2009). It is this diversity and disparity of productivity, as well as indications of change, which makes the Southern Ocean such an important study area, and makes understanding the driving forces behind phytoplankton composition, distribution and abundance so important. Through the analysis of satellite-derived ocean colour of the Southern Ocean it is clear that the Scotia Sea is one of the most productive regions (Korb et al., 2010).

1.2 Currents, Fronts and Water Masses in the Southern Ocean

Antarctica is unique in that it is surrounded by the circumpolar Southern Ocean, which is characterised by a series of fronts and currents, one of which the Antarctic Circumpolar Current (ACC), which is made up of a number of different circumpolar fronts, separated by relatively quiescent zones (Ward et al., 2002), which correspond to distinct water masses (Orsi et al., 1995). These fronts include the Subantarctic Front (SAF), the Polar Front, (PF) and the Southern ACC Front (SACCF). The southern limit of the ACC is demarcated by the Southern Boundary (SACCB) (Orsi et al., 1995). Water masses are identifiable through their distinct physical (Rintoul & Bullister, 1999) and chemical signatures (Zentara & Kamykoski, 1981). These distinct and marked gradients in physical and chemical properties as well as the separation of the water masses by circumpolar current features provide a useful tool with which to interpret observed phytoplankton distributions (Boyd, 2002).

The ACC is a region of low sea surface temperatures (<2 °C) and weak density stratification, as well as receiving little surface irradiance in the summer (Mitchell et al., 1991). Strong wind stress leads to persistently deep mixed layers of >50-80 m which exposes phytoplankton to low irradiance that potentially limits phyto-

plankton growth (Mitchell et al., 1991; Boyd, 2002; Cochlan, 2008). Since the 1990s it has also been known that the ACC is iron depleted (Martin, 1990), resulting in the 'iron hypothesis' (Morel et al., 1991), in which phytoplankton productivity and community composition are controlled by the co-limitation of light and iron. Low light increases cellular Fe demand (Sunda and Huntsman, 1997; Maldonado et al., 1999) and as smaller cells are better adapted to scavenge nutrients at low concentrations (Raven, 1990), low Fe concentrations shift the community towards smaller cells such as mineralisd nanoplankton (Cullen, 1991; Smith and Lancelot, 2004).

All of the above factors combine to create an environment that is unsuitable to support high phytoplankton biomass. Consequently, the Antarctic Circumpolar Current (ACC) is characterised by continually high concentrations of major plant nutrients but low phytoplankton biomass (Mitchell et al., 1991; Pollard et al., 2009).

In both the South Atlantic Ocean and off South Western Australia, the Polar Front (PF) has been consistently associated with increased rates of primary production (e.g. Banse, 1996; Van Franeker et al., 2002). Cubillos et al. (2006) found that the highest cell abundances of coccolithophores were found on the Antarctic Polar Front's southern boundary. The polar front (PF) also acts as a boundary, separating the different morphotypes found within the *Emiliania huxleyi* species where north of the PF one finds only morphotype A, the region south of the PF is populated by the less calcified morphotype B/C (Cubillos et al., 2006).

In the Southern Ocean south of the APF, macronutrient concentrations are generally high, such that they do not limit phytoplankton growth (Boyd, 2002). Approximately half of the nitrate and phosphate in the euphotic zone in the HNLC Southern Ocean is returned unused as the Antarctic Circumpolar Current (ACC) carries surface waters beneath the nutrient poor waters running along its northern rim (Falkowski et al., 1998). Of all the macronutrients, only dissolved silicic acid (dSi) concentrations may become depleted, particularly north of the APF, as it is an essential nutrient for supporting diatom growth (Falkowski et al., 1998).

North of the APF, dSi concentrations may become depleted during diatom blooms stimulated by increased iron availability, which leads to dSi limitation or iron-dSi co-limitation of the phytoplankton community (Frank et al., 2000; Boyd, 2002; Poulton et al, 2007). However, only large diatom species (cells >300 μm in diameter) are positively correlated with increased dSi concentrations, suggesting that these diatoms have high dSi requirements (Poulton et al., 2007). Conversely, small diatom species (<35 μm) sometimes do not flourish despite high dSi concentrations, suggesting that factors other than dSi can control their biomass unlike large diatom species (Poulton et al., 2007).

1.3 Nutrients and the HNLC Condition

Departures from the canonical in situ ambient nutrient ratio of dSi to nitrate (NO_3^-) ratios (dSi:NO_3^-) of 1 is consistent with a system that is iron limited (Gravalosa et al., 2008), since dSi:NO_3^- draw-down rates are influenced by the availability of dissolved iron (Moore et al., 2007a,b). In the Southern Ocean, in iron-replete waters, dSi:NO_3^- ratios are approximately 1:1, whereas in iron deficient waters, the ratio is usually greater than or equal to 2:1 (Boyle, 1998; Smetacek et al., 2004; Moore et al., 2007a,b). HNLC regions such as the Southern Ocean are generally iron limited because they are distant from dominant sources of iron, such as deserts and continental margins. Thus, iron is a major limiting element for phytoplankton growth in the HNLC Southern Ocean. However, in several regions of the Southern Ocean natural iron fertilization occurs in association with shallow bathymetry (e.g., Kerguelen Islands, Blain et al., 2007; Crozet Plateau, Pollard et al., 2009; Scotia Sea, Nielsdottir et al., 2012).

Hinz et al., (2012) have shown that in iron fertilized regions, for example around shallow topographical

features such as islands, phytoplankton assemblages were dominated by large (40 μm to 200 μm) diatoms. On the other hand, small celled nano- and picoplankton (2 μm to 20 μm), which include flagellates, coccolithophores and other small phytoplankton, outcompete large celled phytoplankton in iron deficient waters because of their greater surface area to volume ratio (SA/v), which allows them to scavenge Fe at lower concentrations (Banse, 1996).

While iron availability is important, bloom formation requires favourable light conditions, often provided by some suitable level of water-column stratification (Mitchell et al., 1991). Arrigo et al., (1999) found that in the Ross Sea, phytoplankton community structure was related to the mixed layer depth, and that diatoms tended to dominate in highly stratified waters. Sakshaug and Holm-Hansen (1986) postulated that blooms would only develop in waters with a mixed layer of less than 40 m, but as the ACC has persistent mixed layers in excess of 50 m (Mitchell et al., 1991), this would tend to result in deep mixed layer light-limitation. Mixed layer depths, as little as 10 km apart, varied by as much as 2-fold (Smetacek et al., 2002 and references therein). This type of 'habitat patchiness' caused by frontal dynamics, subjects phytoplankton to a wide range of growth environments over time scales as short as days to weeks - the average period between storms (Smetacek et al., 2002) - and contrasts strongly with the more uniform, deep mixed layers that characterise the ACC south of the APF. Fluctuating growth environments could create favourable growth conditions for a variety of different phytoplankton that respond to differing light regimes due to variable mixed layer depth.

The sea ice margin is another region where blooms can be observed in the Southern Ocean. One reason is due to fresh water stability conferred by melting pack ice in the austral spring and summer. This low-salinity/low density water forms a stable surface layer that confines phytoplankton to the euphotic layer (Walker et al., 1986), allowing phytoplankton to flourish in the well-lit and stable surface waters. However, as vertical mixing increases and the low density water becomes more 'diluted', the phytoplankton bloom dissipates (Walker et al., 1986).

In studies by Murphy (1995) and Ward et al. (2002) in the region of South Georgia, primary and secondary production rates were elevated in the Southern ACC Front. Dense blooms typically occur around South Georgia, but are usually absent in the central Scotia Sea and only moderate in the southern Scotia Sea (Korb et al., 2010). South Georgia is looped anti-cyclonically by the Southern Antarctic Circumpolar Front (SACCF) and is south of the Polar Front (PF), and hence it is strongly influenced by the SACCF as it loops around the island's shelf from the south (Ward et al., 2002). Enhanced production in this area has been linked to increased concentrations of iron in the water derived from the shelf sediments (Boyd et al., 1995; Nielsdottir et al., 2012). In similar ways, productivity around the Kerguelen and Crozet Islands has also been linked to iron availability (Blain et al., 2007; Pollard et al., 2009).

1.4 Phytoplankton Communities

Phytoplankton in the Southern Ocean can be divided into two categories based on their relative sizes and turnover rates (Smetacek et al., 2002). The first category consists of small celled picoplankton (<2 μm) and nanoplankton (2 μm to 20 μm) groups which make up an important component of the microbial food web (Azam et al., 1989). The second category consists of large-celled or chain-forming diatoms and *Phaeocystis*, falling into the microplanktonic (>20 μm) size class (Smetacek et al., 2002). *Phaeocystis* is prevalent where dSi concentrations are low or limiting, but exist in a colonial form where Fe is available (Lucas et al., 2007). Picoplankton and nanoplankton groups are distributed fairly homogeneously throughout the Southern Ocean,

with little seasonal fluctuation in biomass (~0.2 µg chl-*a* L^{-1} to 0.4 µg chl-*a* L^{-1}), whereas microplankton biomass fluctuates widely (~0.5 µg chl-*a* L^{-1} to 5 µg chl-*a* L^{-1}) as a result of temporal shifts in dominance most likely due to local iron/light co-limitation or selective grazing pressure (Smetacek et al., 2002; Moore et al., 2007a,b).

Overall, nanoplankton (2 μm to 20 μm) and picoplankton (0.2 μm to 2 μm) make a significant contribution to production and biomass in the Southern Ocean (e.g., Seeyave et al., 2007; Hinz et al., 2012) by virtue of their widespread and ubiquitous distribution between the circumpolar fronts (Daly et al., 2001; Kang et al., 2001; Boyd, 2002). However, diatoms are the dominant microplankton of the Southern Ocean as they seem to be particularly well adapted to Southern Ocean waters in terms of light, temperature and nutrient availability (Eynaud et al., 1999). Indeed, throughout the Southern Ocean phytoplankton blooms associated with islands such as South Georgia or Crozet are dominated either by diatom species or by *Phaeocystis antarctica* (Korb et al., 2008; Poulton et al., 2007) because of greater iron availability. Where iron is lacking, small cells are favoured, while *Phaeocystis* is generally replaced by diatoms where dSi and iron are available. The heavily silicified *Fragilariopsis kerguelensis* is the dominant diatom taxon in austral HNLC and Polar Frontal waters of the Southern Ocean, although other diatom species may alternate in dominance (Bathmann et al., 1997; Eynaud et al., 1999).

Coccolithophores are an extremely important group of nanoplankton, with a significant role in carbon fixation and the export of organic matter into the deep sea (Poulton et al., 2007b). Occasionally they may account for >20% of the total carbon fixation in unproductive subtropical gyres (Poulton et al., 2007b). The ubiquitous coccolithophore, *Emiliania huxleyi*, is prevalent in surface waters of the ACC north of the APF in summer months (Holligan et al., 2010). The main factors that controls coccolithophore distribution are temperature and irradiance combined with calcite saturation, a function of temperature and changing ocean pH. Even so, *E. huxleyi* has been found in low numbers in much colder waters of <2 °C south of the APF, its presumed and historical southern biogeographical limit (Winter et al., 1994; Eynaud et al., 1999; Holligan et al., 2010). Cubillos et al. (2007) found that compared with historical data, there has been a north–south shift in distribution, which could indicate a response to global climate change.

Coccolithophores are the primary producers of $CaCO_3$ and the production of $CaCO_3$ is thought to increase when diatom growth is limited by either silicic acid or iron (Klaas and Archer, 2002). Klaas and Archer (2002) distinguished three forms of mineral ballast: calcium carbonate, opal and lithogenic material. Transfer efficiency (T_{eff}), the fraction of exported organic matter that reaches the deep ocean, has been found to be positively linked to deep ocean calcite fluxes recovered from sediment traps (Henson et al., 2012). This implies that ballasting by calcium carbonate ($CaCO_3$) may play a role in regulating T_{eff} (Francois et al., 2002; Henson et al., 2012). At high latitudes where diatoms are frequently dominant, export efficiency is usually high (Henson et al., 2012). Coccolithophores are the primary producers of $CaCO_3$ and the production of $CaCO_3$ is thought to increase when diatom growth is limited by the unavailability of silicic acid or iron (Klaas & Archer, 2002).

1.5 Thesis Aims

Traditionally, ship based studies have been considered insufficient by themselves for mapping phytoplankton distribution patterns due to their low spatial and temporal resolution (Sullivan et al., 1993), particularly since extreme environmental conditions in the Southern Ocean can restrict ship access. However in the Weddell Sea, cloud cover greatly restricts satellite imagery, thus making ship based studies in this region an extremely

important tool for understanding phytoplankton spec distribution in this area.

In the Southern Ocean, diatoms and coccolithophores are perhaps the most studied in terms of species composition, but traditional light microscopy techniques used to differentiate between species largely preclude the detection of calcareous taxa such as coccolithophores (Holligan et al., 2010). However, through the use of scanning electron microscopy (SEM), one can achieve a much higher observational resolution and therefore a better level of identification within the smaller size classes such as nanoplankton, as well as calcareous taxa.

This study utilizes SEM to create a clearer idea of the distribution and abundance of the mineralised phytoplankton groups in the Weddell and Scotia Seas and how these trends relate to environmental factors such as temperature, salinity, macronutrient concentrations and mixed layer depth, for example.

The study site and cruise track for this work falls within the South African National Antarctic Programme (SANAP) Bonus Good Hope (BGH) project in the Atlantic Sector of the Southern Ocean between Cape Town and Antarctic (SANAE base), (South African National Antarctic Expedition base) and between SANAE and South Georgia (the 'buoy run').

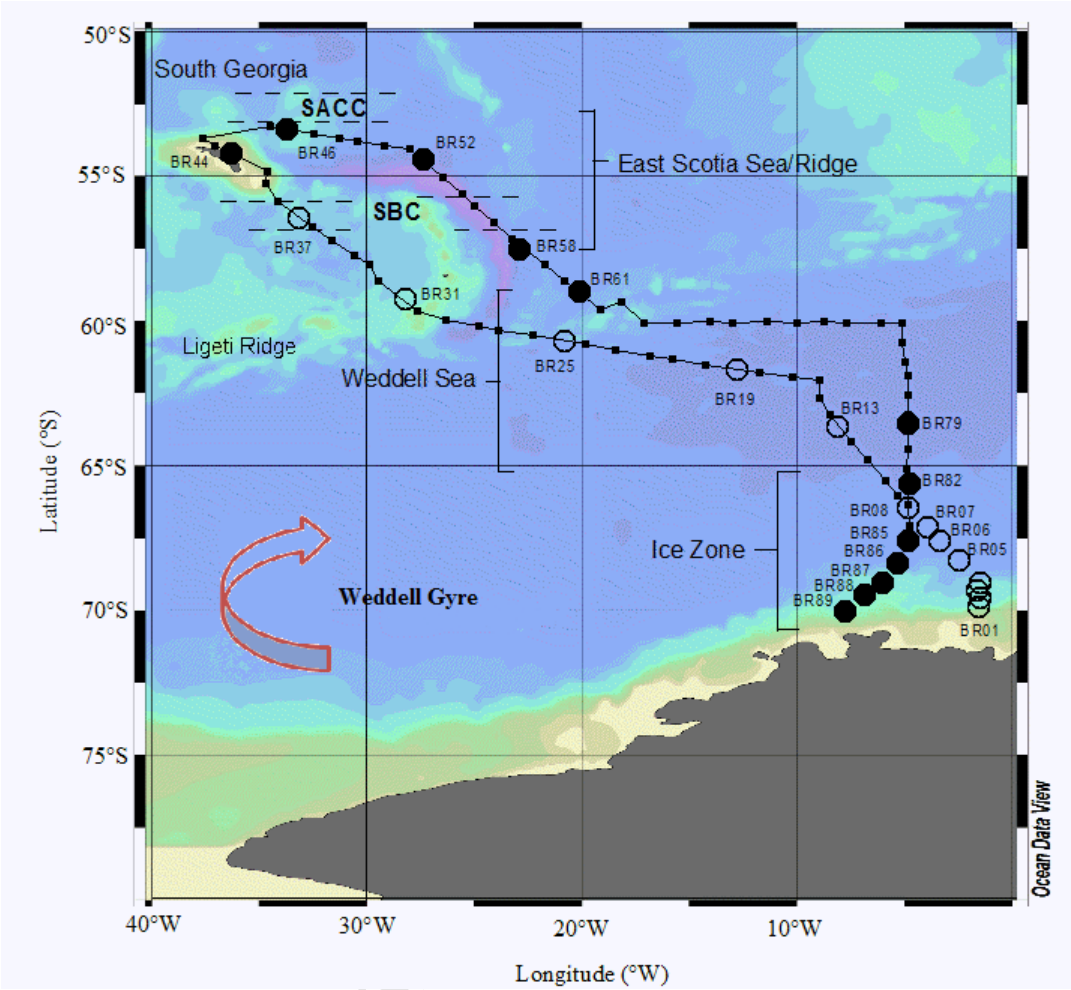

Figure 1: Map of the Cruise track of 'buoy run' (open circles: SEM stations on the northward journey, closed circles - SEM stations on the southward journey, BR05 - BR01 (unlabelled: Stations BR03 and BR04), small circles: other station samples) (colours on map show relative depth of ocean)

1.6 Objectives of Study

The central objective of this study is to examine changes in the mineralised phytoplankton community composition along a 2010 transect between the Scotia and Weddell Seas and how these trends relate to environmental factors. Based on previous work and the literature, three inter-linked hypotheses related to the distribution of diatoms and coccolithophores in this region will be examined:

- Hypothesis 1 (H1): *Mineralized nanoplankton show strong and recognisable distribution patterns across the major fronts and zones in the Southern Ocean, similar to those seen in the east Scotia Sea by Hinz et al. (2012).*

- Hypothesis 2 (H2): *This zonal distribution pattern is linked to shared/different growth-limiting environmental factors, and that these factors - such as the availability of silicic acid and sea surface temperatures (SST) - are responsible for observed patterns of distribution.*

2 Methods

2.1 Cruise Details and Sampling

The data set was collected during the December 2009–February 2010 cruise of *MV* SA Agulhas, SANAE 49. This thesis focuses on the data collected during the 'buoy run' leg of the cruise (16 January 2010–10 February 2010), from the ice shelf to South Georgia and back, a transect that crosses the Weddell Gyre and the Scotia Sea (Figure 1). The SANAE 49 cruise track crossed four distinct oceanic domains: the seasonal, marginal ice-edge zone; the permanently open ocean zone; the shelf zone of the South Sandwich and South Georgia Islands; and the frontal zones of the Antarctic Polar Front, the Sub Antarctic Front, and the Sub Tropical Front. The 'buoy run' leg of the cruise provided the main focus of the biogeochemical observations. Both underway and water column sampling using a CTD and inline messenger triggered bottles were used to collect water samples. A CTD was deployed twice daily at 09:00 hours and 21:00 hours and 10 depths (5m, 10m, 30m 40m, 50m, 60m, 100m,200m, 350m and 500m approximately) were sampled. Engine room seawater samples were collected from a depth of approximately 5m daily at 02:00hours, 06:00 hours, 14:00 hours and 18:00 hours. During the second leg of the buoy run, due to a spate of bad weather the ship was forced to change course and stations BR62 - BR74 were sampled along 60 degrees South due to a spate of bad weather. This bad weather was followed by the first period of sun in weeks.

2.2 Scanning Electron Microscopy (SEM)

The composition of the mineralised phytoplankton community was examined using SEM analysis of filtered seawater samples. Seawater samples used for SEM analysis were collected from the engine room tap with an inlet approximately 5m below the ship. To filter the seawater samples, 1-2 L was measured out and gently vacuum-filtered through a 1 µm pore size, 25 mm diameter Cyclopore polycarbonate filter (backed with a 0.5 µm Cyclopore polycarbonate filter). The filtration pump was run for 2–4 hours, with the majority of filters being removed after two hours and the volume filtered was then measured and recorded.

After filtration, the filters were rinsed using pH-adjusted MilliQ (pH ~10) to prevent the formation of salt crystals, which makes analysis by SEM difficult. Filters were then oven-dried at ~45 °C for ~7 hours and placed in Petri dishes, wrapped in tin foil and kept in a cool, dry place for future analysis. Silica crystals were placed in the storage container to ensure samples stayed dry.

Back in the laboratory ashore, 25 random stations were selected (due to the expense of running the SEM) and samples were mounted on SEM aluminium pin stubs and sputter coated with 20 nm of gold. Secondary electron microscope images of sample fragments were obtained on a LEO1450VP (variable pressure) SEM equipped with a Princeton Gamma Technology (PGT) light element energy dispersive X-ray microanalysis system (EDS). Imaging was undertaken using the following settings: 5kV, a probe current setting of 30oA, and a working distance of 8 mm. For cell counts, a 15 x 15 frame grid was imaged and archived according to a tailored macro at a constant 5000x magnification. Each species in the 225 fields of view (FOV) per filter were identified and counted. Species identification followed Tomas (1997) and Scott and Marchant (2005).

Biomass data of phytoplankton in terms of carbon equivalents was estimated using methods seen in Poulton et al, (2007a) and Hinz et al. (2012).

2.3 Ancillary Measurements

Discrete underway samples were taken for nutrients (NO_3^- and SiO_4^{4-},), chlorophyll-*a*, flow-cytometry and microscopy.

Temperature

Temperature profiles were derived from XBT (eXpendable Bathy Thermograph) deployments, from daily CTDs, and from an underway pCO_2 system – the latter being used in this study and matched to the 'buoy run' stations using time, latitude and longitude.

Salinity

Salinity samples were collected from the uncontaminated underway laboratory supply and from selected depths from CTD casts, as well as from the Underway Conductivity, Temperature and Depth profiler (UCTD) and pCO_2 system. CTD salinity samples were stored in acid-washed, 250 ml salinity bottles for later analysis on a porta cell at UCT. These samples were used to calibrate the UCTD. During the cruise, the UCTD salinity sensor cracked and therefore salinity measurements from the UCTD were not used. Instead, conductivity measurements were taken from the pCO_2 system and matched to the 'buoy run' stations using time, latitude and longitude co-ordinates, which were then converted to salinity (Fofonoff and Millard, 1983).

Nutrients

Nitrate (NO_3^-), silicic acid (SiO_4^{4-}), phosphate (PO_4^{3-}), ammonium (NH_4^+) and urea measurements were made according to the manual method described in Grasshoff et al., (1983) and Parsons et al., (1984). Nutrient samples BR60 to BR77 were stored frozen (-20 °C) and analysed on the homeward bound leg of the cruise 2-4 days later. Only nitrate and silicic acid were used in the final analysis due to issues with the mass spectrometer which occurred during the cruise.

Chlorophyll-*a*

Seawater samples (250 ml) for chlorophyll-*a* (Chl-*a*) measurements were run through 25 mm Whatman GF/F filters (effective pore size 0.7 μm). After filtration, the filters were placed in 8 ml 90% acetone to extract the Chl-*a* in a dark fridge overnight. Chl-*a* in the filtrate was measured using a Turner Designs fluorometer, calibrated with fresh Chl-*a* standard (Sigma, UK), and set up to measure Chl-*a* in the presence of chlorophyll-*b* using Welschmeyer (1994) filters.

MLD

The MLD was determined using the de Boyer Montégut et al. (2004) temperature criterion. The MLD was identified where temperature changed by 0.2°C, relative to a reference value at 3m depth.

2.4 Statistical Analysis of Count and Environmental Data

Statistical approach used in this thesis was developed during attendance of a training course in multivariate statistics. It is important to note that due to the multivariate nature of the data, multivariate analysis is the only way to analyse this data. Phytoplankton counts (cells ml^{-1}) were analysed using the multivariate programme E-PRIMER (Plymouth Routines In Multivariate Ecological Research, version 6.1.6) (Clarke and Gorely, 2006), with count data transformed using a fourth root transformation due to the high variation in abundance between samples (between 0 cells ml^{-1} and approximately 5000 cells ml^{-1}). Between-station differences were calculated based on all species present regardless of what contribution each species made to the total biomass, as rare species may be characteristic of specific areas or water masses (Korb et al., 2012).

A Bray-Curtis similarity matrix was calculated before applying hierarchical Cluster analysis and ordination via Multi-Dimensional Scaling (MDS) with the aim of identifying relationships between samples. Cluster analysis created a dendrogram, which provides a measure of similarity of phytoplankton samples. A SIMPROF analysis (1000 permutations, 5% significance level), which tests for evidence of structure in an a priori unstructured set of samples (Clarke and Gorely, 2006), was then run to determine the significance of the station

groupings. The Cluster analysis and MDS plots revealed that Station BR44 (South Georgia) was completely different in composition from the rest of the stations, and was therefore excluded from further analysis.

From these relationships, pre-determined environmental indices were created *a priori* to try and link phytoplankton groups with different environmental conditions. These *a priori* environmental indices were established using the raw data matrix and included:

- Oceanic zones (Ice, Open water and Shallow/Coastal water)
- Temporal variations in sampling (northward transect, southward transect)
- Water Mass (north of 60°S and south of 60°S)

Labelling of the MDS with these environmental indices (Oceanic Zones, Sampling variability and Water mass) allowed examination of how these related to trends in the mineralised phytoplankton community structure. ANOSIM, which summarises patterns in species composition and environmental variables (Clarke and Gorely, 2006), was then used to test whether the indices chosen created significant groups or not. As Zones and Temporal indices were found to be insignificant, only the index 'Water Mass' was utilized from this point on.

SIMPER, which is used to identify the species primarily providing the discrimination between two observed sample clusters (Clarke and Gorley, 2006), was then run using the rectangular data matrix with the added 'index' column which was previously determined to be significant using ANOSIM. Only those species which were the main contributors (80% of dissimilarity) were listed (so as to remove any bias from rare species which could skew the distribution). SIMPER created a list of the species that characterized each group (based on environmental index), which was previously defined by the indices listed through the cluster analysis. It also provided a list of species that best separated each pair of groups specified by the index column. Rare species contributing little (<5% of total biomass) to overall biomass were removed.

Diversity indices were also calculated based on standardised biomass and included was the number of species (N), the Shannon-Weiner diversity index (H'), and Pielou's evenness (J') index. Shannon-Weiner diversity indicates both the relative species richness and the degree to which biomass is evenly distributed between species. Pielou's evenness indicates only how evenly the biomass is distributed among the different species, without accounting for the species richness. Pielou's evenness ranges between 0 and 1, with a low value indicating that the population is not evenly distributed amongst the different species with perhaps one or two species dominating the biomass, and a high value indicating an even spread of biomass between species.

Environmental data collected included temperature, salinity, Chl-*a* concentration, as well as nitrate and silicic acid concentrations. These data exist (for the most part) for all 89 stations sampled along the 'buoy run', although silicic acid data are missing for seven stations. Two sets of environmental data were analysed. The first consisted of abiotic data for all 89 'buoy run' stations. Stations that had missing data points (silicic acid) were removed from the analysis so that 81 stations were included in this analysis. The aim of this analysis was to determine which environmental variables will have driven the distribution of stations relative to one another. Five Principal Components (PCs) were analysed and associated eigenvectors were used to provide an estimate of the relative weight of the environmental variables in the sample data (Clarke and Gorley, 2006). Principle Components Analysis is utilised to identify statistical trends in data based on eigenvector decomposition of a covariance matrix (Clarke and Gorely, 2006).

The second set of environmental data was a subset which matched the SEM abundance stations. The aim of this analysis was to generate Principal Components of environmental data with which to do a BEST test. The

BEST routine in E-PRIMER works by linking multivariate biotic patterns to suites of environmental variables to determine which environmental variables are most likely driving the observed pattern in the SEM abundance distribution (Clarke and Gorely, 2006). Environmental data were first analysed using draftsman plots to determine what kind of transformation to apply to the data, and to determine if all the data needed to be transformed in the same way. The data were then normalized because of the different units used. As the data were mostly normally distributed, it was decided not to apply any further transformation to the data. Lastly, the environmental data were then analysed using Principal Component Analysis (PCA) to determine relationships based on the environmental data between the different samples/stations. The BEST algorithm was then used to determine the 'best' match between the two multivariate among-sample patterns determined earlier in the analysis (namely MDS for the biotic variables and PCA for the abiotic variables). BEST was carried out using the BIO-ENV method because the number of environmental variables is not very high and therefore it was more feasible to run the BIO-ENV option over the BVSTEP. BIO-ENV examines all possible combinations of variables, from each environmental variable separately, through to all at the same time, thus if there are a large number of environmental variables this method can be too time consuming. BVSTEP, alternatively, first fits the environmental variable with the strongest relationship and then adds in the variable with the next strongest relationship and is therefore run when the number of environmental variables is too high to run BIO-ENV, as in this case.

3 Results

3.1 General Oceanography

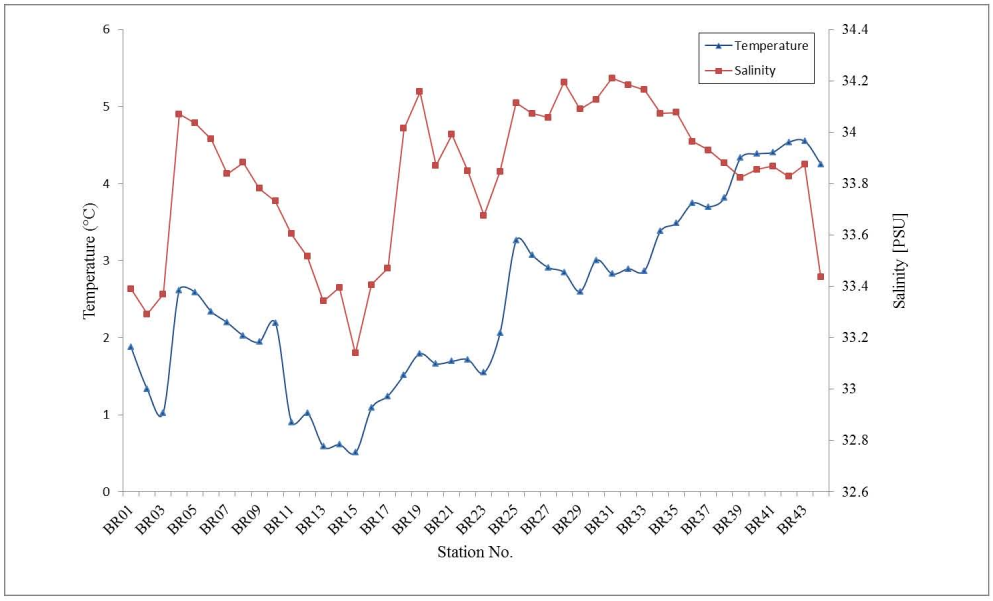

(a)

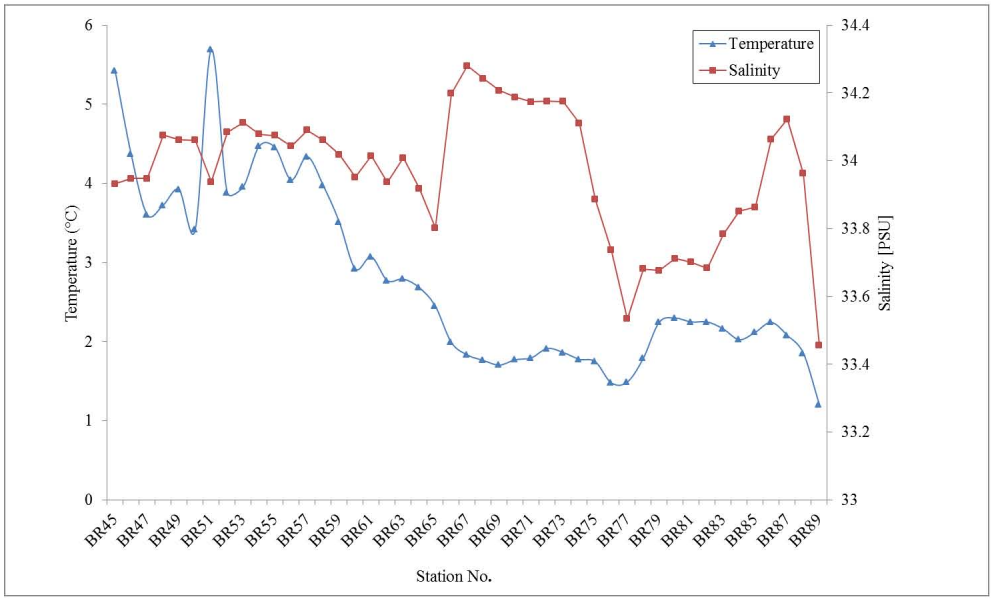

(b)

Figure 2: a) Plot of surface temperature (°C) and salinity measurements for stations sampled during leg 1 of the 'buoy run' (Stations BR01 - BR44), b) Plot of surface temperature (°C) and salinity measurements for stations sampled during leg 2 of the 'buoy run' (BR45 - BR89) (the data has been plotted as equally spaced samples from BR01 to BR89 rather than linearly against latitude).

There was a strong Sea Surface Temperature (SST) gradient along the 'buoy run' (Figure 2), with SST ranging from ~0.75 to 1.5 °C to the south of 60°S, and north of 60°S towards South Georgia from ~1.5 to ~4.5 °C. Around South Georgia, there was a large increase in SST to ~6 °C, with Station BR44 located within Stromness Sound. Salinity also fluctuated along the 'buoy run', varying from ~33.2 to ~33.4 as the cruise's track passed between saline and fresher waters, the latter presumably due to precipitation or ice melt.

Temperature was generally low (~2 °C) at higher latitudes (south of 60°S), whereas silicic acid concentrations (dSi) were generally ~40 μmol L^{-1} (Figures 2 and 3). Conversely, where SST was higher than ~4-6 °C in the vicinity of South Georgia, dSi was 50% lower than in other areas (10-20 μmol L^{-1}). At Station BR44, dSi reached the lowest value found on the 'buoy run' (0.96 μmol L^{-1}), corresponding to a SST of around 6 °C (Figures 2 and 3). SST and dSi are strongly correlated with a R^2 value of 0.54 ($p < 0.001$, n=81). Relative to the variability in dSi, nitrate concentrations were far less variable and generally ~20 µmol L^{-1} regardless of latitude (Figure 3). Exceptions were found at Station BR01 (10 µmol L^{-1}) and at Stations BR33, 85 and 89 (all ~25 µmol L^{-1}). This variability in dSi relative to more consistent nitrate (NO_3^-) concentrations means that the dSi:NO_3^- ratios range between 3.8 at BR01 and 0.05 at station BR45 (Figure 3). The ratio of dSi to NO_3^- draw-down in the Weddell Sea was typically >2:1, with the exception of Station BR03 and Station BR15. However in the Scotia Sea dSi:NO_3^- ratios were predominantly ~1:1 or lower. From Station BR34 to Station BR57 draw-down ratios were all 1:1 or lower.

In Figure 4a, mixed layer depths (MLDs) were generally shallower south of latitude 60°S (average, ± standard deviation; 25.8 m, ± 5.3 m), whereas as the 60°S boundary was approached, MLDs deepened rapidly by ~20 m, after which there appeared to be a fairly significant overall deepening of the MLD to ~50 m. Mixed layer depths were shallower at the beginning of the 'buoy run' (60°S) and also at South Georgia. In Figure 4b, the same pattern appears, with MLD generally deeper to the south of South Georgia, but deepening nearer to 60°S. There was also a sharp deepening in MLD just south of 60°S, although lower latitudes appeared to have generally shallower MLD (30.6 m ± 4.9 m). There is no significant difference in MLD between buoy runs or North and Southward legs. The average is different, however there is too much variability to be a significant difference. The MLDs are highly variable, potentially due to mesoscale effects and difficulties in describing the mixed layer dependent on temperature/salinity. density when both temperature and salinity are influential and their influence differs with latitude.

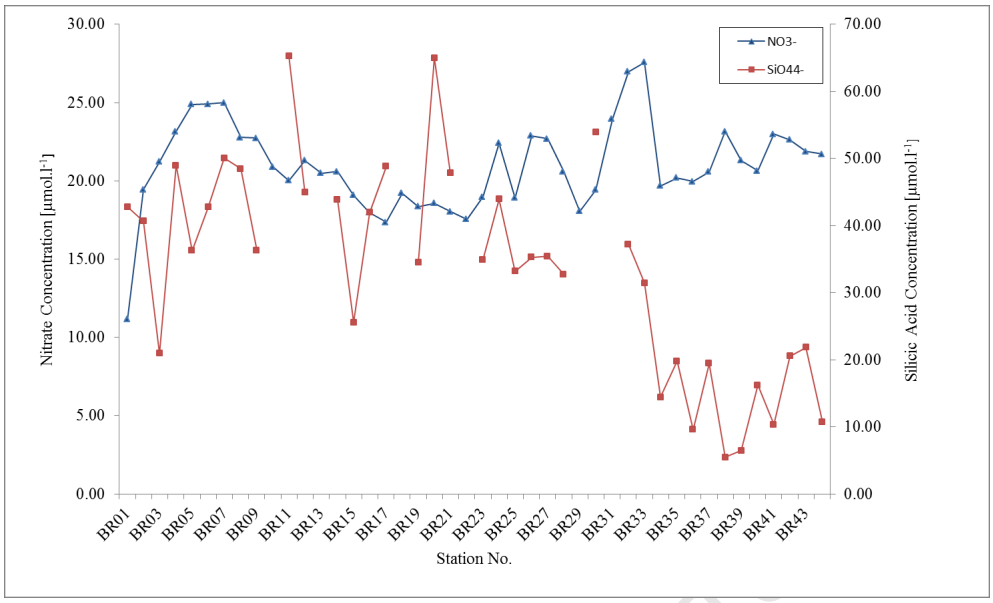

(a)

(b)

Figure 3: a) Plot of nitrate (µmol L^{-1}) and silicic acid (µmol L^{-1}) concentrations during leg 1 of the 'buoy run' (stations BR01-BR44), b) Plot of nitrate (µmol L^{-1}) and silicic acid (µmol L^{-1}) concentrations during leg 2 of the 'buoy run' (BR45-BR89) (the data has been plotted as equally spaced samples from BR01 to BR89 rather than linearly against latitude).

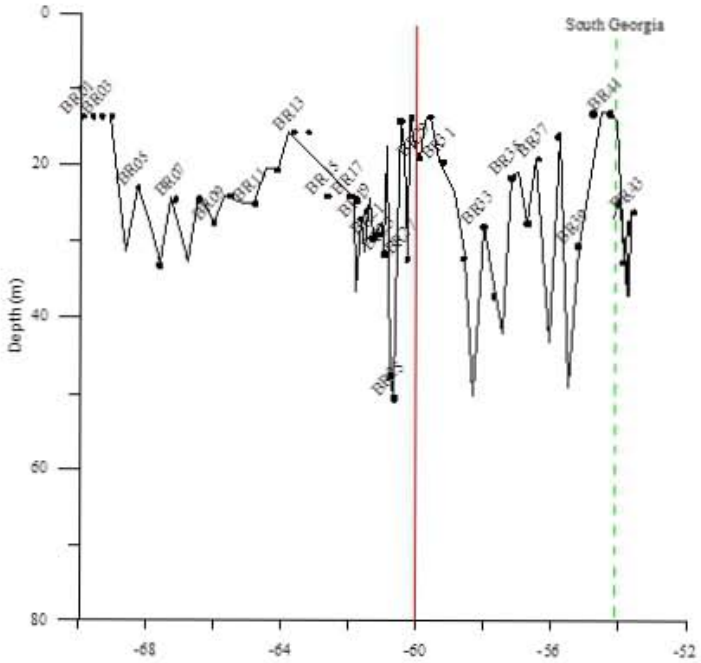

(a)

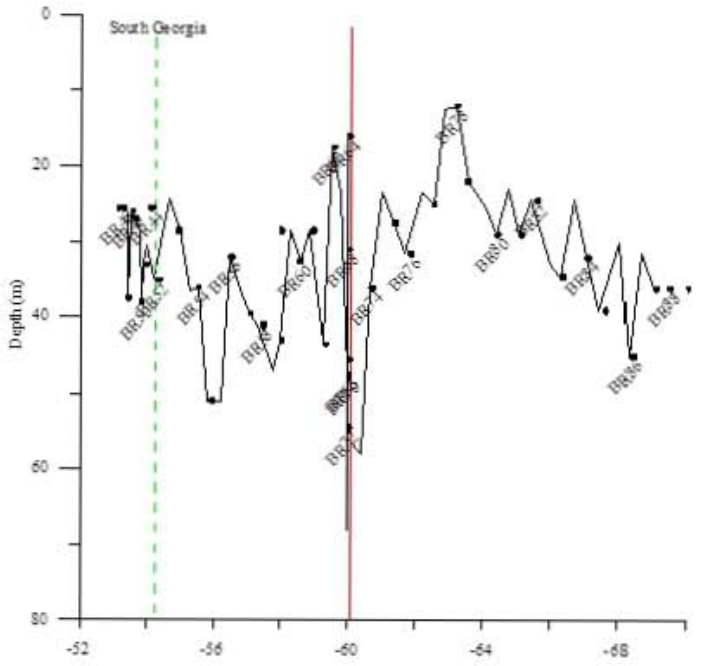

(b)

Figure 4: (a) Mixed layer depth (MLD) for the northward leg of the buoy run. (b) Mixed layer depth (MLD) for the southward leg of the buoy run. Note that the 60°S line indicates where the ship followed 60°S latitude due to bad weather.

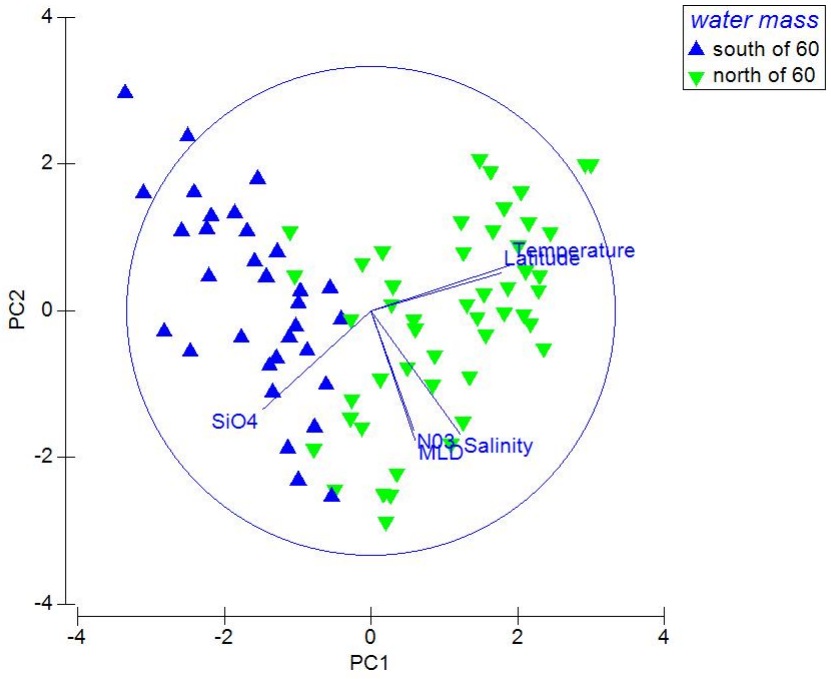

(a)

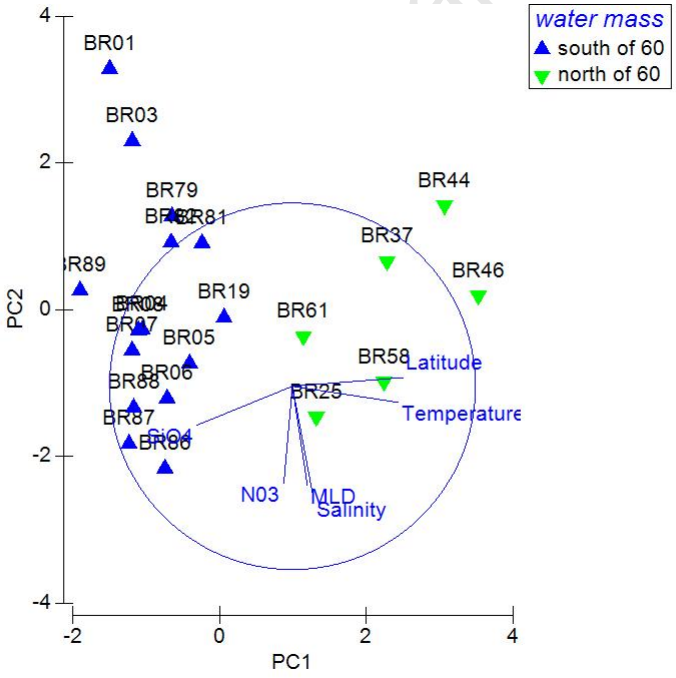

(b)

Figure 5: (a) PCA of environmental variables which include; latitude, NO_3^-, SiO_4^{4-}, temperature, salinity and MLD illustrating the observed pattern when all 89 'buoy run' stations are utilized. (b) PCA of environmental variables which include; latitude, NO_3^-, SiO_4^{4-}, temperature, salinity and MLD. (Shows only the stations which correspond to abundance stations).

Table 1: Eigenvectors for each environmental variable used in the abiotic PCA analysis. Eigenvectors are provided individually for each PC.

Environmental Variables	PC1	PC2	PC3
Latitude	0.606	0.011	0.121
NO_3^-	-0.073	-0.657	-0.713
SiO_4^-	-0.536	-0.183	0.441
SST	0.577	-0.163	0.119
Salinity	0.082	-0.713	0.518

PCA (Principle Components Analysis) was used to consider which environmental variables could be determining phytoplankton distribution before further analyses were run. Figures 5a and 5b show a clear distinction between stations situated south of 60°S (Weddell Sea) and north of 60°S (Scotia Sea). PC1 accounted for 51.1% of the variation and PC2 accounted for 30.1% of the variation. The largest eigenvectors for PC1 was latitude, closely followed by temperature. The largest eigenvector for PC2 was salinity followed by nitrate. Accounting for 13% of the variation, PC3 eigenvectors were not considered because PC1 and PC2 described more than 80% of the variation.

3.2 Phytoplankton Community Composition

Small Fragilariopsis (Figure 6b) were the numerically dominant species of mineralised phytoplankton sampled at nearly every station, with the exception of Stations BR44, BR46 & BR52 and BR58, which were dominated by *Corethron pennatum* (Figure 6e) (33.33%), *Chaetoceros* sp. (small) (Figure 6d) (78.56%, 55.55%), and *Tetraparma pelagica* (Figure 6a) (52.10%), respectively. Small *Fragilariopsis* sp. (i.e. between 5 µm and 20 µm) were ubiquitous, making up the majority of the diatom population at most sample sites (Figure 6). In this study, small *Fragilariopsis sp*. were on average slightly more abundant in the Weddell Sea than in the Scotia Sea. Medium-sized *Fragilariopsis* sp. (20 µm-40 µm), which are classic HNLC diatoms (Smetacek et al., 2004), were more commonly found in the Weddell Sea. Small *Chaetoceros* sp. (<10 µm) were also present throughout the 'buoy run', but were predominantly found in the Scotia Sea surrounding South Georgia at Stations BR52 and BR58, *E. huxleyi* coccoliths (Figure 6a) had the highest abundance (coccoliths per ml) and Station BR58 had the highest abundance of *E. huxleyi* cells, as well as the highest abundance of *Tetraparma pelagica* overall.

Station BR52 had the highest number of species (22) and Station BR44 (South Georgia) the lowest (6). Similarly, BR44 had the lowest total number of individuals at 18 cells ml^{-1} and Station BR89 had the highest total number at 5,646 cells ml^{-1}. With respect to evenness (how evenly the individuals are distributed among the different species), individuals within the sample from Station BR44 were not evenly distributed, with one species dominating (*Corethron* sp., see Table 2) the total (86.46%). Station BR05 exhibited a much more even distribution, while Station BR44 exhibited the lowest species richness and diversity, whereas Station BR05 showed the highest.

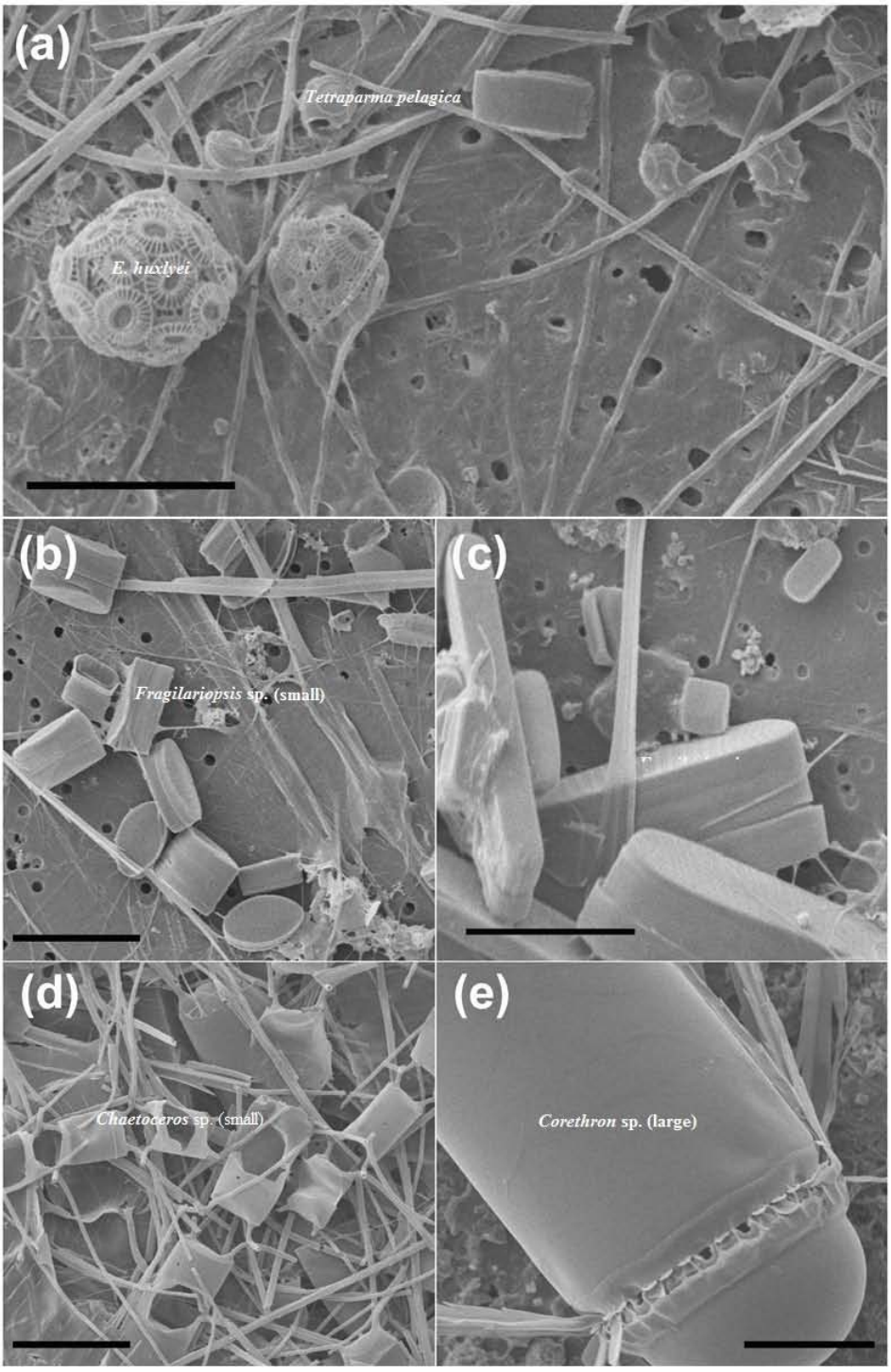

Figure 6: SEM images of major species found: a) *Emiliania huxleyi* (left hand side) and *Tetraparma pelagica* (right hand side), b) *Fragilariopsis sp.* (small), c) *Fragilariopsis sp.* (medium), d) *Chaetoceros sp.* (small), e) *Corethron sp.* (large). Scale bars: a-e =10 µm.

Table 2: Phytoplankton data (diatom abundance, diatom diversity (S, total number of phytoplankton (diatoms and non-diatom species); J' - Pielou's evenness), dominant species, *E. huxleyi* abundance, *E. huxleyi* coccolith abundance, *Tetraparma pelagica* abundance).(**E. huxleyi* coccoliths highest numerically, but not a 'species').

Station No.	Diatom Abundance	Community Diversity		Dominant sp.	*Emiliania huxleyi*	*E. huxleyi* coccoliths	*Tetraparma pelagica*
	(cells per ml)	S	J'		(cells per ml)	(coccoliths per ml)	(cells per ml)
BR01	1183.00	1203.5	0.32	*Fragilariopsis* sp. (Small) (**76.78%**)	0	1.61	0
BR03	1768.76	1801.6	0.38	*Fragilariopsis* sp. (Small) (**64.30%**)	0	0	0.57
BR04	429.30	429.8	0.69	*Fragilariopsis* sp. (Small) (**32.83%**)	0	0	0
BR05	2066.18	2076.7	0.21	*Fragilariopsis* sp. (Small) (**89.35%**)	0	0.92	5.51
BR06	1102.18	1105.9	0.28	*Fragilariopsis* sp. (Small) (**83.52%**)	0	0	1.38
BR07	1512.77	1536.0	0.22	*Fragilariopsis* sp. (Small) (**88.22%**)	0	0	16.83
BR08	446.06	457.0	0.45	*Fragilariopsis* sp. (Small) (**67.23%**)	0	0	5.79
BR13	1088.96	1112.7	0.63	*Fragilariopsis* sp. (Small) (**35.72%**)	0	0	0.99
BR19	1167.35	1169.8	0.63	*Fragilariopsis* sp. (Small) (**44.58%**)	0	0	0
BR25	1144.01	1777.9	0.62	*Fragilariopsis* sp. (Small)* (**34.72%**)	138.23	1592.75	485.87
BR31	1686.12	1803.0	0.51	*Fragilariopsis* sp. (Small) (**57.53%**)	0	0.91	116.93
BR37	1391.11	1417.6	0.27	*Fragilariopsis* sp. (Small) (**82.50%**)	8.68	122.93	15.08
BR44	17.46	17.5	0.86	*Corethron pennatum* (Large) (**33.33%**)	0	0	0
BR46	1550.53	1559.6	0.29	*Chaetoceros* sp. (Small) (**78.56%**)	4.09	105.1	1.36
BR52	945.86	976.4	0.52	*Chaetoceros* sp. (Small) (**55.55%**)	8.34	329.34	12.51
BR58	775.21	2265.1	0.53	*Tetraparma pelagica**(**52.10%**)	266.16	2036.19	1180.02
BR61	1844.00	2693.6	0.42	*Fragilariopsis* sp. (Small) (**56.00%**)	57.58	492.65	790.61
BR79	2012.65	2027.0	0.59	*Fragilariopsis* sp. (Small) (**55.46%**)	0	0	2.87
BR81	3693.07	3710.8	0.58	*Fragilariopsis* sp. (Small) (**51.37%**)	0	0	5.33
BR82	1282.38	1307.6	0.60	*Fragilariopsis* sp. (Small) (**52.88%**)	0	0	1.48
BR85	1022.30	1035.6	0.51	*Fragilariopsis* sp. (Small) (**57.16%**)	0	0	1.84
BR86	1720.80	1825.0	0.36	*Fragilariopsis* sp. (Small) (**76.46%**)	0	0	0.93
BR87	3151.83	3167.0	0.25	*Fragilariopsis* sp. (Small) (**83.65%**)	0	0	12.39
BR88	2704.07	2717.8	0.20	*Fragilariopsis* sp. (Small) (**88.91%**)	0	1.83	6.4
BR89	5622.47	5646.2	0.26	*Fragilariopsis* sp. (Small) (**82.87%**)	0	0	5.48

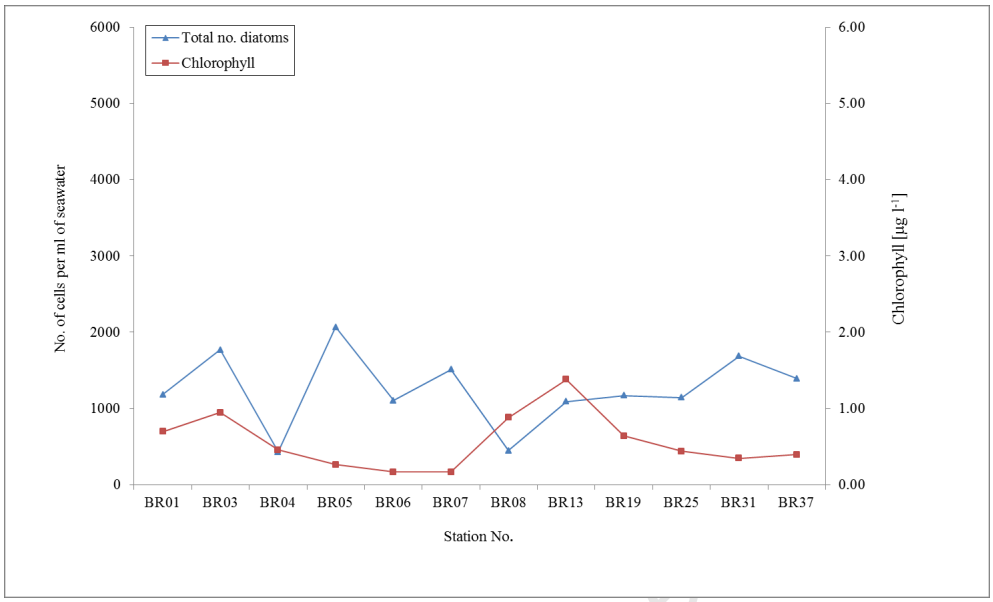

(a)

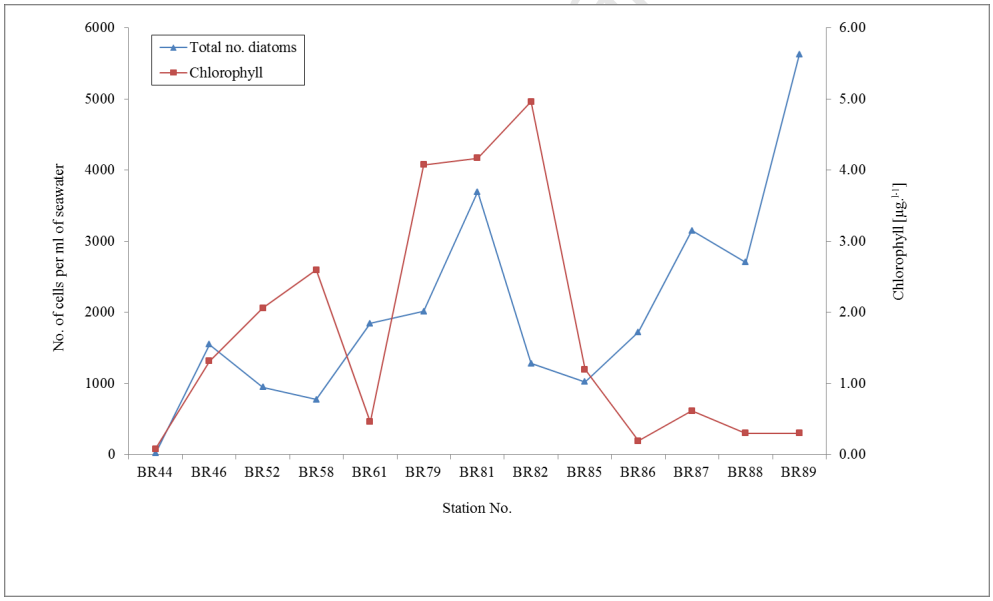

(b)

Figure 7: a) Plot of the total number of diatoms per ml of seawater per station sampled and corresponding Chlorophyll-*a* (Chl-*a*) concentrations ($\mu g\ L^{-1}$) for leg 1 of the 'buoy run' (BR01-BR44), b) Plot of the total number of diatoms per ml of seawater per station sampled and corresponding Chlorophyll-*a* (Chl-*a*) concentrations ($\mu g\ L^{-1}$) for leg 2 of the 'buoy run' (BR45-BR89).

In general, Chl-*a* appeared to be lower at stations where the numbers of diatoms were high, (BR05, BR06,

BR07, BR31, BR37, BR61, BR87, BR88 and BR89). However, at certain stations (BR52, BR59), Chl-*a* concentrations were high where diatom numbers were low. Chl-*a* concentrations were very low (0.08 µg L^{-1}) at Station BR44 where the total number of diatom cells per ml was also very low (<20 cells ml^{-1}). This was true also for Stations BR04 and BR09. The highest concentration of Chl-*a* was at Station BR81 (4.96 µg L^{-1}) and the lowest at Station BR50 (0.05 µg L^{-1}) (Figure 7). Chl-*a* concentrations rose steadily from Station BR41 to Station BR81 across the 60°S latitude. At the start and end of the 'buoy run' (at the stations closest to the ice), Chl-*a* concentrations were generally low (<0.5 µg L^{-1}), while at the midway stations (between the ice and South Georgia), Chl-*a* concentrations were generally higher (>1.0 µg L^{-1}). The station with the highest abundance of diatoms was Station BR89, with 5,622 cells ml^{-1}. By contrast, the station with the lowest number of diatoms was Station BR44 (sampled within the fjord at South Georgia), with just 18 cells ml^{-1}.

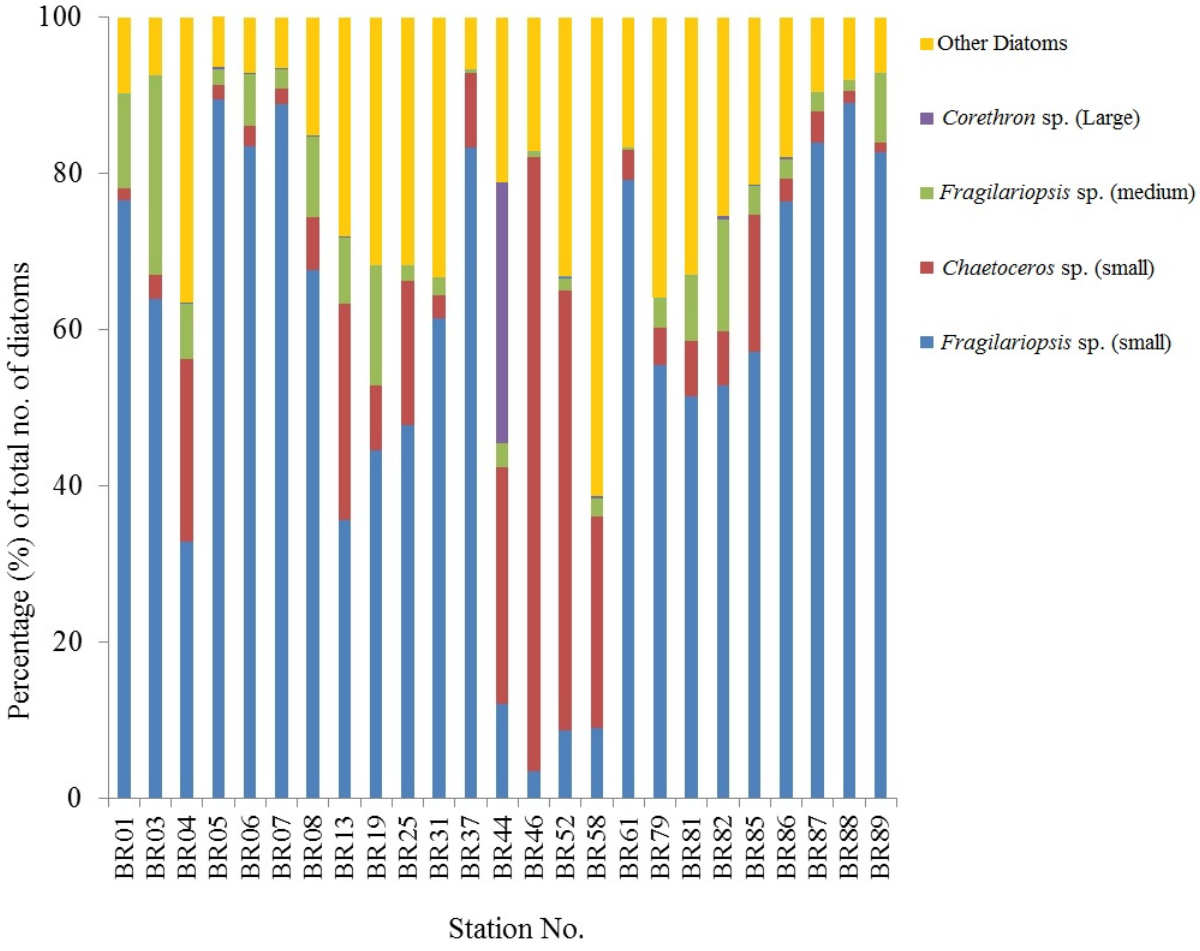

Figure 8: Stacked bar chart showing the four diatom species found in the highest numbers overall as percentages of the total.

Small *Fragilariopsis* sp. (~5 – 20 µm) were found at every station sampled during the 'buoy run' in high proportions, apart from stations at and surrounding South Georgia. At these stations (BR46, BR52 and BR58), small *Chaetoceros* sp. (<10 µm) were dominant. However, the dominant species at Station BR44 (sampled within the fjord at South Georgia) was *Corethron pennatum* and this was the only station where it appeared as a dominant/prominent species. Medium sized *Fragilariopsis* sp. (20 – 40 µm) were also found at every station sampled (Figure 6).

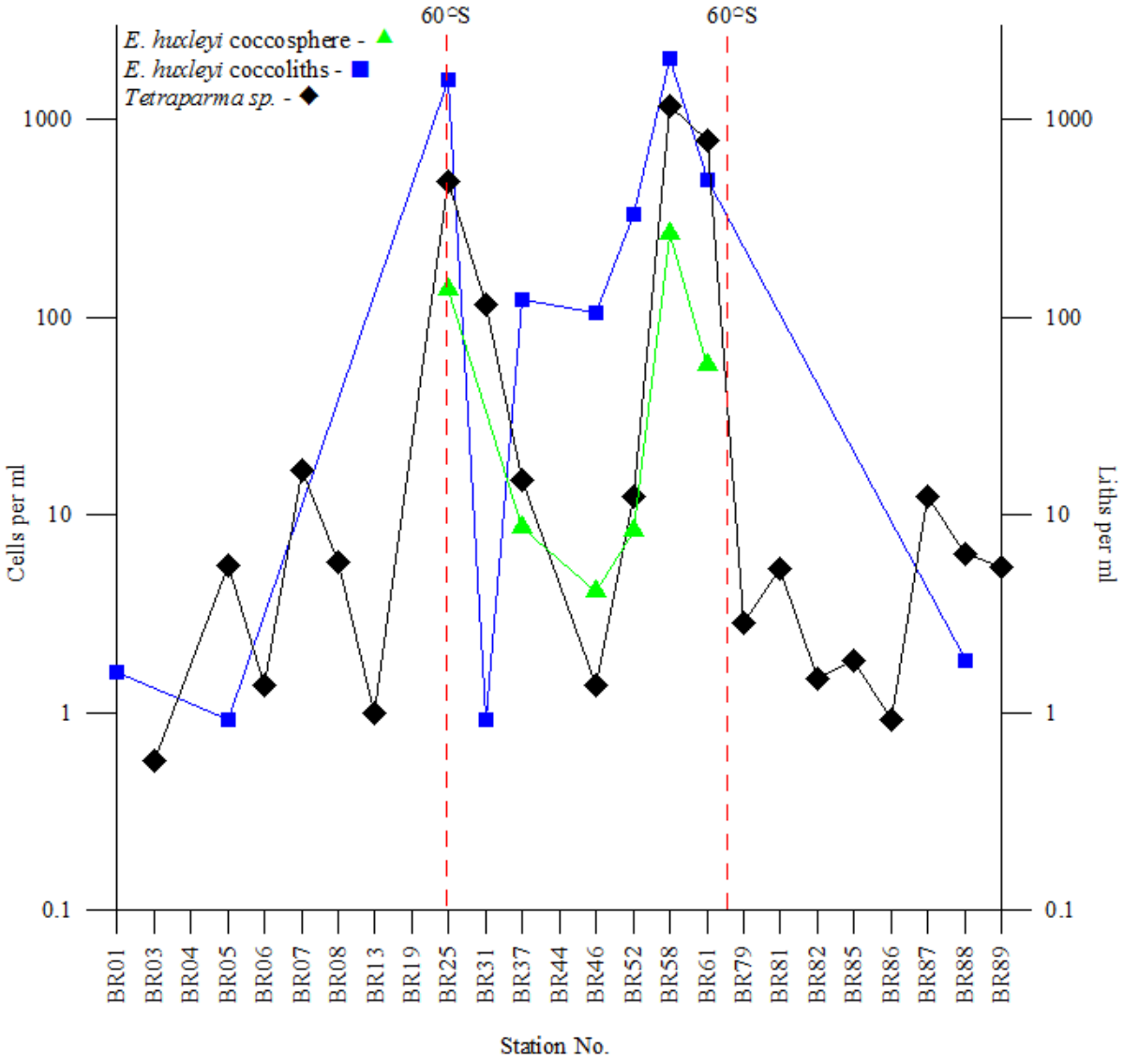

Figure 9: Plot comparing the abundance and distribution of *Emiliania huxleyi* (coccoliths and coccospheres) and *Tetraparma pelagica* on the 'buoy run'.

The chrysophyte *Tetraparma pelagica* was distributed more widely between the Weddell and Scotia Seas, but was generally found in lower abundances in the Weddell Sea compared with the Scotia Sea. *Tetraparma pelagica* abundance peaked at 60°S on both the northward and southward legs of the 'buoy run', and its abundance resembled that of the coccolithophorid *Emiliania huxleyi*. While *Emiliania huxleyi* coccospheres were found only north of 60°S, a few detached coccoliths were found close to the ice. *Emiliania huxleyi* coccospheres and coccoliths, as well as *Tetraparma pelagica*, peaked at the Scotia-Weddell boundary (Ligeti Ridge).

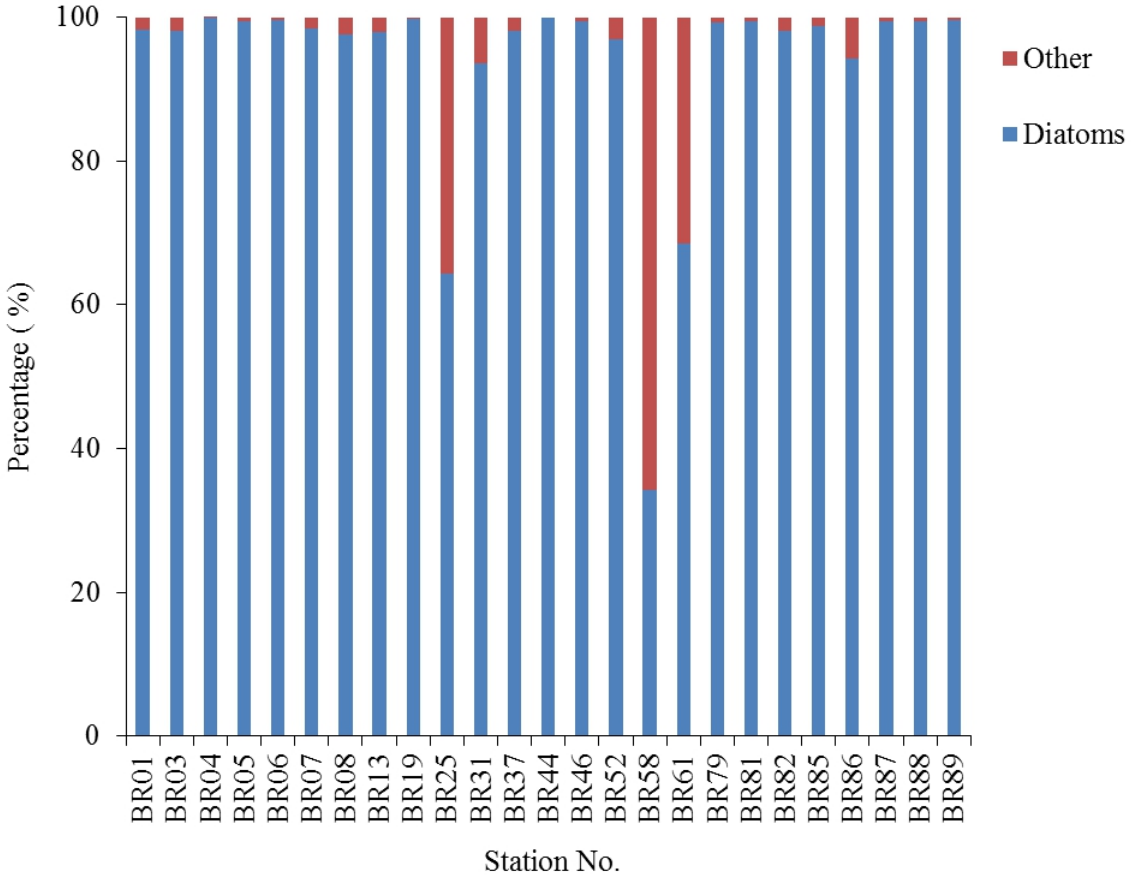

Figure 10: Stacked bar chart showing what proportion of the mineralised phytoplankton community at each station can be attributed to diatoms versus 'other' ('other' includes *Emiliania huxleyi, Dictyocha* sp.*, Tetraparma* sp.*, Prorocentrum* sp. and cysts).

Diatoms were the dominant group at every station sampled except at Station BR58, which fell in the east Scotia Sea. Generally there was a higher proportion of non-diatom species found in the east Scotia Sea when compared with stations in the Weddell Sea. Biomass from the cell counts ranged from 27.95 mg C m^{-3} at Station BR01 to 478.68 mg C m^{-3} at Station BR25. Furthermore, as can be seen in Figure 11a, at all stations

Table 3: SIMPER results (Cut off for low contributions: 80%) (North of 60 Group (east Scotia Sea): BR25–BR61; South of 60 Group (Weddell Sea): BR01–BR19, BR79–BR89). Average similarity for North of 60 group is 60% and average similarity for the South of 60 group is 76.33%.

Groups south of 60 & north of 60						
Average dissimilarity = 38.06						
Species	Group south of 60	Group north of 60	Av.Diss	Diss/SD	Contrib%	Cum.%
	Av.Abund	Av.Abund				
Fragilariopsis sp. (small)	5.73	4.11	3.3	1.03	8.67	8.67
Tetraparma pelagica	1.12	3.01	3.04	1.43	8	16.67
E. huxleyi	0	1.88	2.44	1.43	6.41	23.08
Cylindrotheca sp.	2.52	1.94	2.24	1.21	5.88	28.95
Fragilariopsis sp. (medium)	3.17	1.86	2.02	1.19	5.31	34.26
Nitzschia sp.	2.64	1.75	1.89	1.07	4.96	39.22
Chaetoceros sp. (small)	2.95	3.66	1.87	1.3	4.9	44.13
Thallossisiosira sp.	0.52	1.58	1.79	1.79	4.71	48.84
Pseudonitzschia sp.	1.77	2.18	1.75	1.31	4.6	53.44
Rhizosolenia sp.	1.53	1.58	1.63	1.17	4.27	57.71
Cysts	1.14	0.1	1.56	1.71	4.09	61.8
Dictyocha sp.	1.47	0.87	1.5	1.11	3.95	65.75
Fragilariopsis sp. (large)	1.56	0.88	1.36	1.07	3.58	69.34
Corethron sp. (small)	1.47	0.9	1.32	1.12	3.48	72.81
Chaetoceros sp. (medium)	2.35	2.31	1.29	1.28	3.4	76.21
Dactyliosolen sp.	0.71	0.65	1.26	1.09	3.31	79.52
Chaetoceros sp. (large)	1.23	0.63	1.26	1.21	3.31	82.83

sampled during the 'buoy run', small cells (i.e. between 5–20 µm) were dominant. The medium size class is the next most dominant group. However, with respect to cell carbon (Figure 11b), large cells (>1000 pg C cell^{-1}) appeared to be dominant at nearly every station with the exception of a few stations closest to the ice: BR01, BR03 and BR89 where small cells (0–99 pg C cell^{-1}) were dominant. The medium size (100–999 pg C cell^{-1}) class represented a very small proportion of the phytoplankton community at each station. The small size class represented between 0 and 60% of the total community at each station.

The cluster dendrogram based on community composition (Figure 12) separated stations out as follows: BR31, BR25 and BR61 (left hand side, green box, henceforth described as cluster A), stations situated in 'Open Ocean (the Weddell Sea and east Scotia Basin), and Stations BR01 and BR03 were stations closest to the ice at the beginning of the 'buoy run' (Ice Zone). The largest group (Stations BR06, BR19, BR08, BR04, BR82, BR79, BR81, BR13 and BR85) were all close to the ice (Ice Zone), both on the northern and southern legs of the study. A fourth group containing Stations BR05, BR89, BR86, BR87, BR07 and BR88 were also close to ice (Ice Zone). The final group (BR37, BR58, BR46 and BR52, right hand side, green box, henceforth

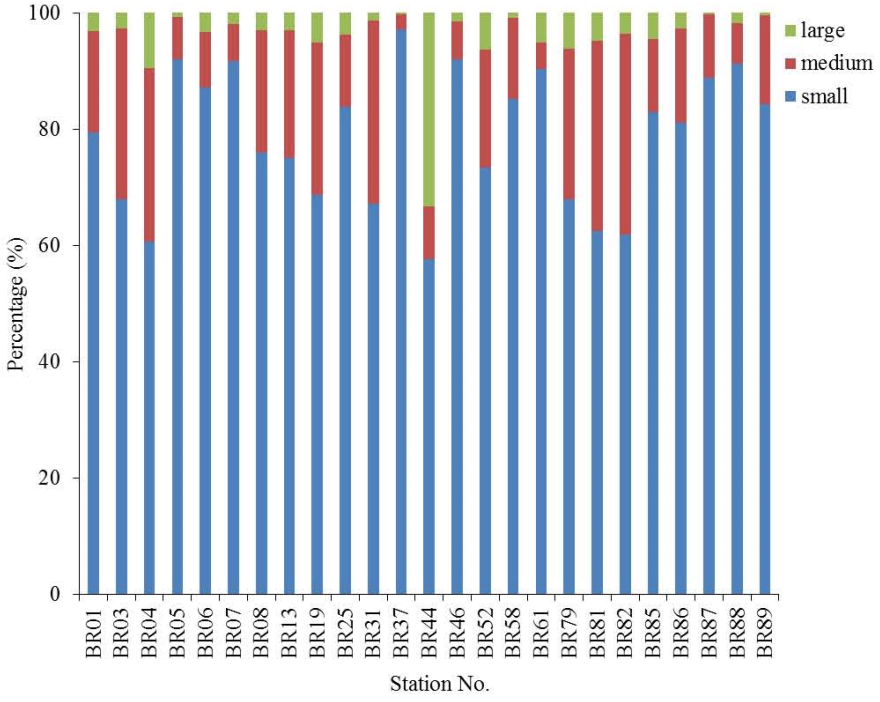

(a)

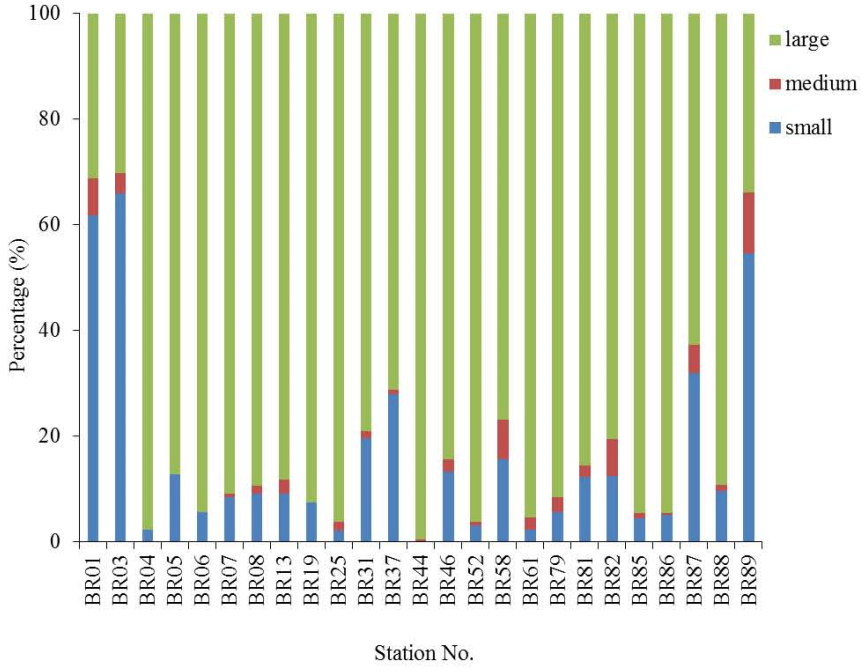

(b)

Figure 11: (a) Stacked bar graph of the proportion of small, medium and large cells at each station (size based on cell length) (small cells: 5–20 µm, medium cells: 20–40 µm, large cells: >40 µm). (b) Stacked bar graph of the proportion of small, medium and large cells at each station based on cell carbon (small cells: 0–99 pg C l^{-1}, medium cells: 100-999 pg C l^{-1}, large cells: >1000 pg C l^{-1}).

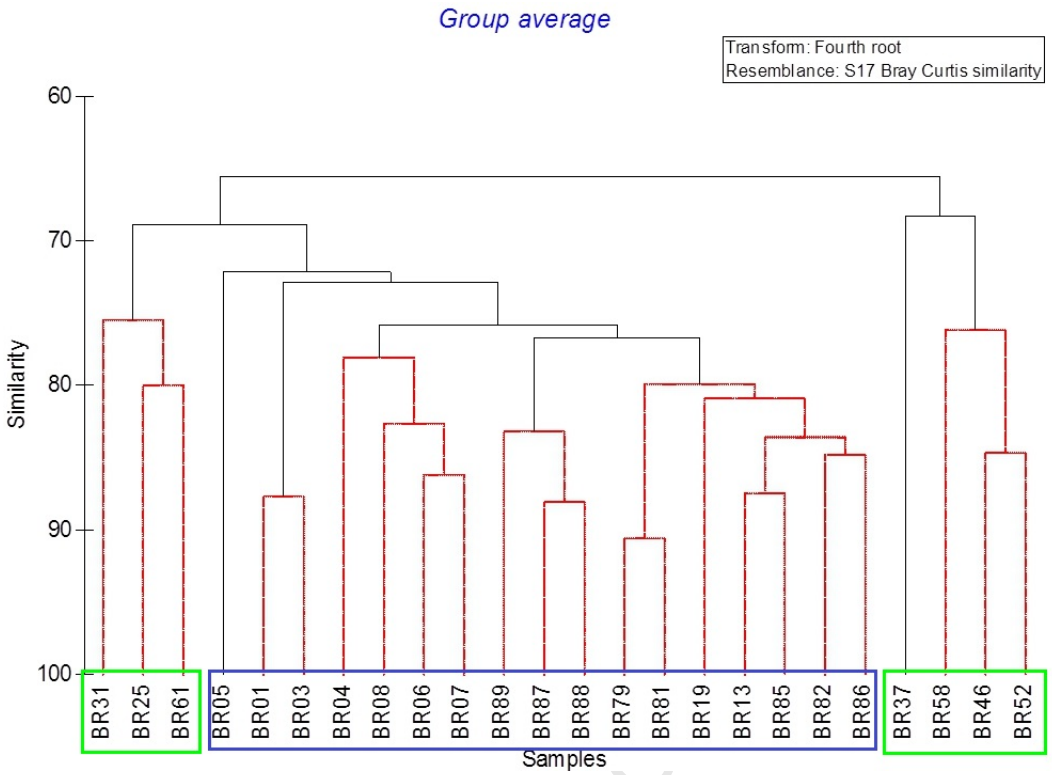

Figure 12: Cluster diagram showing division of stations in the 'buoy run' (excluding Station BR44 which skewed the data distribution) (red denotes significant groups) (green boxes on left and right hand side of cladogram denote stations situated north of 60 degrees, clusters A and B respectively, blue box denotes stations situated south of 60 degrees).

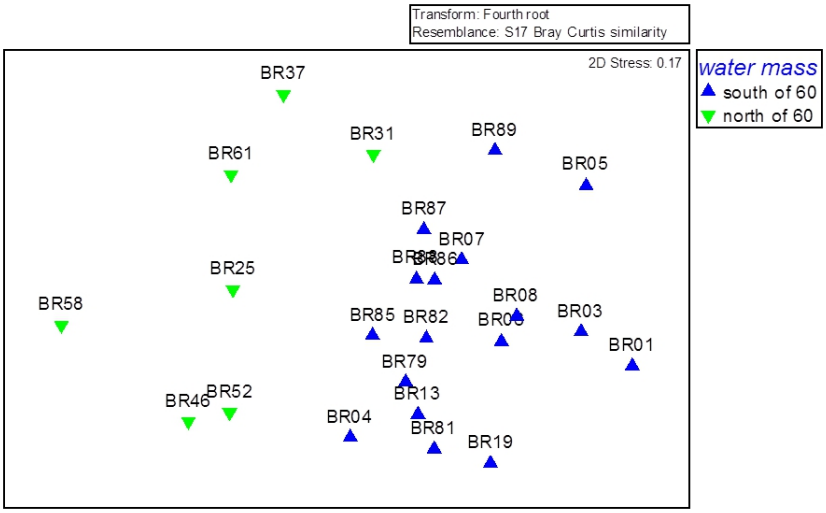

Figure 13: MDS plot of abundance data with the added factor 'region'.

Table 4: BEST results showing correlations for all 5 single variables, the top 2 correlations are highlighted in bold.

No.Vars	Corr.	Selections
2	**0.722**	**1,4**
3	**0.698**	**1,3,4**
1	0.679	4
2	0.649	3,4
4	0.617	1,2,3,4
4	0.614	1,3-5
1	0.612	1
3	0.61	1,2,4
3	0.605	1,4,5
2	0.59	1,3

Variables
1 - Latitude
2 - $N0_3^-$
3 - SiO_4^{4-}
4 - Temperature
5 - Salinity

described as cluster B) were all stations found relatively close to South Georgia (east Scotia Basin and South Georgia). A MDS ordination (Figure 13) of the similarity matrix used in the cluster analysis shows that there was a clear separation between stations that occur in water masses south of 60°S (stations depicted by blue triangles in Figure 13 and enclosed in a blue box in figure 12) and stations that occur north of 60°S (stations depictd by green triangles in figure 13 and clusters A and B in figure 12) (close to South Georgia). There was also more dispersion amongst the shallow/coastal group when compared with the ice region, such that stations in the shallow/coastal group are less similar to each other than stations within the more southern group are to each other; however there are fewer of these stations.

The significance of the index, 'water mass' was tested *a priori* (ANOSIM test). The sample statistic (Global R) of 0.698 had a significance level of 0.1% and therefore the null hypothesis is rejected, and there is a significant difference between stations situated north and south of 60°S.

SIMPER analysis shows that the 'north of 60' region has an average similarity of 76.3% and that the 'south of 60' group has an average similarity of 60%, whereas the two groups are on average 38.1% dissimilar (Table 3). *Emiliania huxleyi* and *Tetraparma pelagica* were only present in the 'north of 60' group and explain 14.41% of the difference between regions. However, small *Fragilariopsis* sp. were more influential in differentiating the two regions, with these species being more abundant in Scotia Sea than Weddell Sea.

Comparison of the patterns in community composition (MDS) with trends in the environmental data (PCA) via the BEST test reveals that the best correlation between the observed patterns in biotic abundance and the environmental variables is provided by two parameters (Table 4), latitude and temperature, which provide a Spearman correlation value of 0.72 ($p < 0.001$). Alternatively, the addition of the variable silicic acid also provides a strong correlation (0.70, $p < 0.001$) (Table 4).

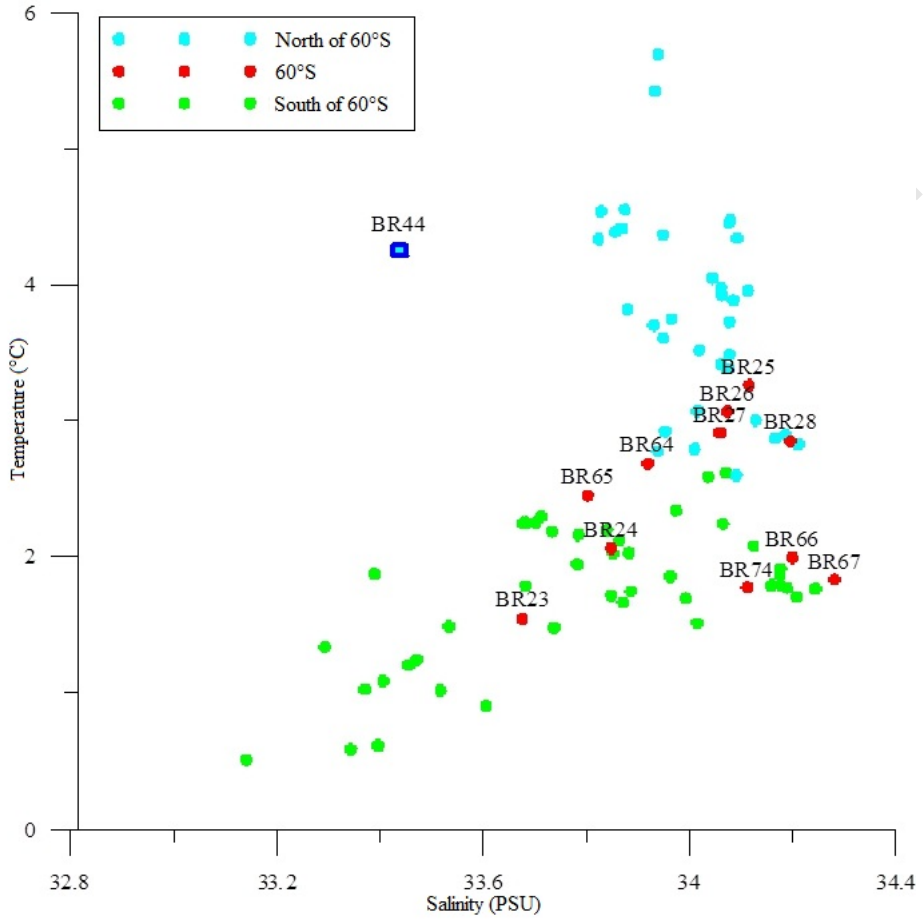

Figure 14: Temperature, salinity plot illustrating how the sampled stations fall into different water masses, those north of 60°S and those south of 60°S. The stations in red were sampled on or very close to the 60°S line, Stations BR64-BR67 and BR74 were sampled along the 60°S line when the ship made a detour due to bad weather (R^2= 0.1696, y = 1.8796x - 61.086).

4 Discussion

4.1 Environmental Drivers of Distinct Phytoplankton Communities

The data was analysed holistically, with little or no pre-conditioning which allows the data to tell it's own story. Cluster and MDS analyses detected two distinct phytoplankton communities (Figures 12 and 13): the first to the South of the Ligeti Ridge was characterised by cooler, fresher waters most likely due to sea-ice melt, and the second to the north of the Ligeti Ridge, which comprised waters that were progressively warmer and saltier (Figure 14). This differentiation of mineralised phytoplankton communities was based on changing environmental gradients that occurred with latitude, the most influential being SST and dSi. Sea surface temperature and dSi are inversely proportional to each other ($p<0.0001$), with high SST correlating ($R^2 = 0.54$) with low dSi values (Figures 2 and 3). Thus, at lower warmer latitudes, dSi availability was generally lower than at higher colder latitudes such as in the east Scotia Sea.

While dSi concentrations south of the Ligeti Ridge were higher on average than those sampled further north, nitrate (NO_3^-) concentrations remained fairly consistent throughout the 'buoy run', leading to a very variable dSi:NO_3^- ratio (Figures 2 and 3). The drawdown of dSi in the east Scotia Sea was presumably driven by increased diatom growth stimulated by iron availability, most likely due to the numerous seamounts and oceanic islands (Korb et al., 2010). Increased iron availability in HNLC waters like the Southern Ocean often facilitates considerable diatom growth, which in turn depletes dSi and leads to dSi limitation or iron-dSi co-limitation of diatom growth (Boyd, 2002; Poulton et al., 2007). Depleted dSi in the east Scotia Sea may be evidence for the role of diatoms drawing dSi down during the early phases of the annual bloom (Poulton et al., 2007a). Examples of this include a massive draw down of dSi at Station BR44, close to South Georgia and a natural source of iron, whereas dSi was highest along the boundary between the Weddell and east Scotia Seas. Station BR44 is significantly different from all other stations along the 'buoy run', most likely due to it being sampled in the bay of South Georgia, such that it falls into an entirely different water mass (Figure 14).

In the Southern Ocean, iron-replete waters are characterised by dSi:NO_3^- uptake ratios of ~1:1 (Poulton et al., 2007a) and iron-deficient waters (HNLC) are characterised by uptake ratios of >2:1 (Boyle, 1998; Smetacek et al., 2004; De Baar et al., 2005). An uptake ratio of ~1:1 is the ratio at which Fe-replete diatoms take up dSi and NO_3^- (Hutchins and Bruland, 1998; Takeda, 1998; Franck et al., 2000). The east Scotia Sea was generally characterised by uptake ratios characteristic of iron-replete waters whereas farther south, in the Weddell Sea, most stations exhibited uptake ratios of greater than 2:1, which implies that waters were iron deficient. Higher dSi:NO_3^- drawdown ratios in iron deficient regions may show a selection for more heavily silicified diatom taxa (Smetacek et al., 2004), for example Station BR44 is completely dominated by large phytoplankton (>1000 pg C cell^{-1}), a large proportion of which were *Corethron* sp., which is heavily silicified and has high iron requirements. Conversely, in an iron-rich environment, Station BR44 exhibited a very low dSi:NO_3^- ratio.

In the Ross Sea, Arrigo et al. (1999) found that phytoplankton community structure was related to the mixed layer depth, such that diatoms were more dominant in strongly stratified water. The mixed layer depth (MLD) in this study was generally shallower in the Weddell Sea, but deepened to the north, in the east Scotia Sea. Poulton et al. (2007a) found that when the mixed layer depth was shallow, it facilitated light-dependent iron uptake sourced from the Crozet plateau. Earlier, Sakshaug and Holm-Hansen (1986) also suggested that blooms would only develop in a well-lit mixed layer of less than 40 m. In the Weddell Sea, mixed layers were shallower than 40 m, whereas in the east Scotia Sea and close to and around 60°S, or the Ligeti Ridge, mixed

layers were frequently deeper than 40 m (Figure 4). In the Weddell Sea, where ice extent is significant and fairly extensive, summer surface waters are stabilised by low-density fresh water, which results in the observed shallower mixed layers (Walker et al., 1986) and resultant higher biomass of diatom-dominated communities. In the east Scotia Sea, north of 60°S, waters were generally more turbulent, resulting in a deeper mixed layer. Critical depth analyses by Nelson and Smith (1991) and by Boyd (2002) suggest that low irradiances associated with deep mixed layers restrict phytoplankton growth throughout much of the growth season in the Southern Ocean, resulting in low biomass of non-diatom taxa.

4.2 Major Phytoplankton Provinces in the east Scotia-Weddell Seas

The stations that were sampled were fairly widely dispersed, from stations sampled in the extreme South amongst the pack ice to those sampled much further North within the bay of South Georgia (Figure 1). In the data, this boundary is also marked by a taxonomic shift, with *Emiliania huxleyi* and *Tetraparma pelagica* occurring in the Scotia Sea, but not in the Weddell Sea (Figure 13, Table 2). Thus, the two groups can be described as falling into two different oceanic provinces: the east Scotia Sea north of the Ligeti Ridge, and the Weddell Sea south of this point. The Scotia Sea is known to have high productivity relative to the Southern Ocean as a whole (Whitehouse et al., 2012), whereas the more southern Weddell Sea is described as a classic high nutrient low chlorophyll (HNLC) zone of lower productivity.

Previously, *E. huxleyi* was known to have a northerly distribution, in which the Antarctic Polar Front was thought to be the southernmost boundary of coccolithophore occurrence (Eynaud et al., 1999). However, coccolithophores have been found to occur much further south, but often only in very low numbers (Winter et al., 1998). *E. huxleyi* is widespread during the summer months in surface waters of the ACC north of the APF (Holligan et al., 2010). At high latitudes, low temperatures are thought to exert the main control on the biogeographical distribution of coccolithophores, however, in the Southern Ocean, frontal systems and hence nutrient distribution are also crucial (Gravilosa et al., 2008). Therefore, a combination of warmer temperatures and available iron could account for the occurrence of *E. huxleyi* in the island dotted Scotia Sea, but not further south in the iron-depleted Weddell Sea. *E. huxleyi* has also been reported in cooler waters (<2 °C) further south than the APF, but generally in low abundances (Holligan et al., 2010).

E. huxleyi was found in highest abundances along the boundary between the Weddell and Scotia Seas, at approximately 60°S, concurrently with highest silicic acid concentrations. Classically, one might therefore expect diatoms to be favoured rather than coccolithophores. Hinz et al. (2012) found, however, that there was a negative relationship between *E. huxleyi* and silicic acid availability, but with no physiological mechanism for this negative correlation, it is unlikely that the two are related, thus the co-occurrence of high *E. huxleyi* abundance with high silicic acid availability is not important. It is possible that *E. huxleyi* cannot flourish further south of this latitude due to increased grazing pressure or perhaps due to cooler temperatures and calcite under-saturation (Hinz et al. 2012).

Phytoplankton species composition differed only slightly between the Weddell and Scotia Sea communities; in fact the species making up cumulatively 50% of the abundance in each water mass were extremely similar. The exceptions were *Tetraparma pelagica* occurring only in the Scotia Sea, *E. huxleyi* occurring much more numerously in the Scotia Sea and *Nitzschia sp*. occurring more frequently in the Weddell Sea. Thus, species

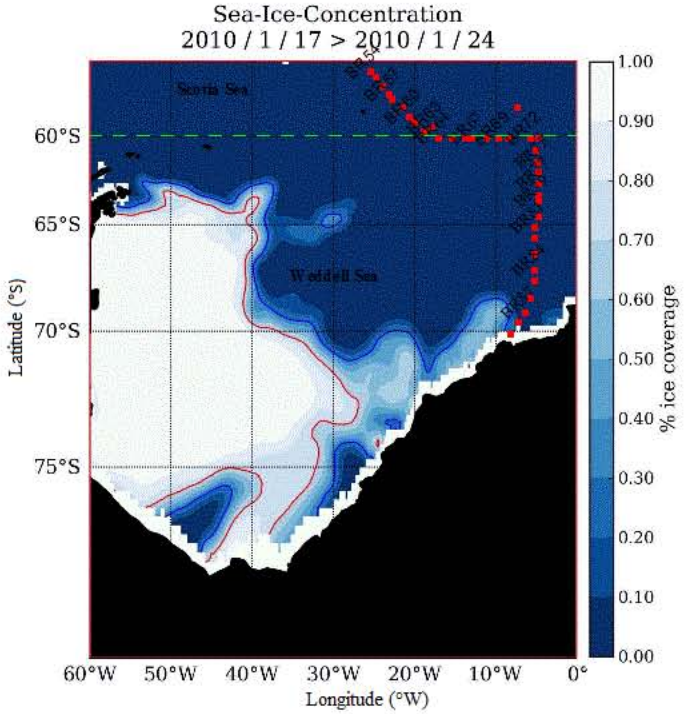

(a)

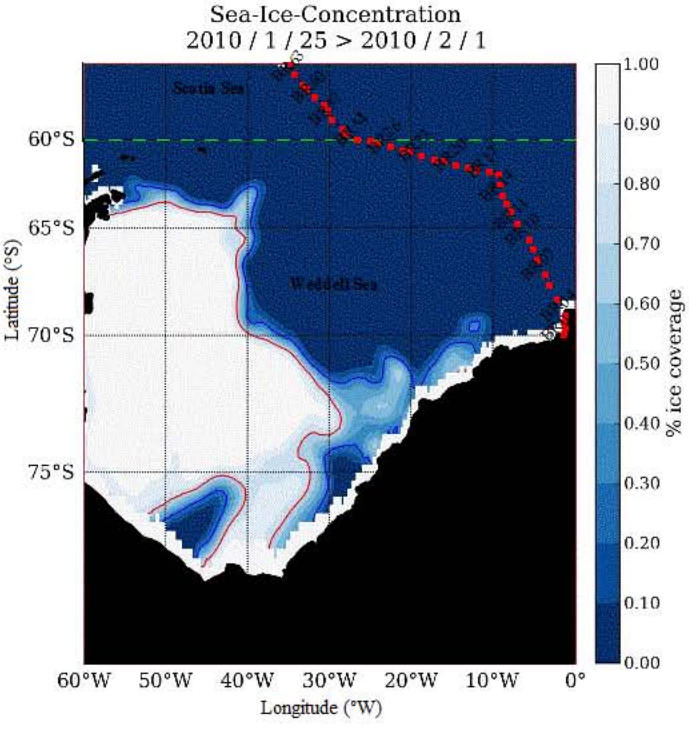

(b)

Figure 15: a) Sea-Ice Concentrations in the Weddell Sea, during the northward leg (leg 1) of the 'buoy run' b) Sea-Ice Concentrations in the Weddell Sea, during thethe southward leg (leg 2) of the 'buoy run' (data from SMMR and SSM/I ICE CONCENTRATION datasets).

abundances varied between the two water masses, but species composition was fairly similar. Walker et al. (1986) found that there was little noticeable difference between ice algae and pelagic communities with respect to phytoplankton species composition, and that species abundance was where the two communities differed most. Ward et al. (2012) found that in two phytoplankton groups, one within the seasonal sea-ice zone and the other north of the Southern Antarctic Circumpolar Current Front, the differences were apparent at the population level, rather than at the taxonomic level. The first group of plankton (within the seasonal sea-ice zone) were persistently low in abundance and biomass, however, the second group (situated north of the SACCF) had consistently higher biomass and abundance.

4.3 Community Trends

In this study, diatoms were the dominant phytoplankton assemblage found throughout the Weddell and Scotia Seas (except at Station BR58, where the total proportion of diatoms was only ~35%). Diatom species differ widely and significantly in their growth requirements, behaviour and life cycle strategies (Smetacek, 1985), as well as in their nutrient requirements. Thus, different diatoms are able to occupy the various niches in the Southern Ocean fairly successfully despite widely ranging nutrient availability, temperatures and salinities (Poulton et al., 2007a). In general, the east Scotia Sea stations had slightly higher proportions of non-diatom species than those found in the Weddell Sea (Figure 10).

Hinz et al. (2012) found a similar pattern to this study, where small *Fragilariopsis* sp. occurred everywhere, but were more numerous at the more southern stations. In iron-replete conditions, such as theoretically found in the Scotia Sea, there was a general shift in phytoplankton community structure from one dominated by picoplankton to one dominated by nano- and microplankton (Moore et al., 2007b).In general, Chl-*a* appeared to be lower at stations where the numbers of diatoms were high, (BR05, BR06, BR07, BR31, BR37, BR61, BR87, BR88 and BR89). However, at certain stations (BR52, BR59), Chl-*a* concentrations were high where diatom numbers were low. Chl-*a* concentrations were very low (0.08 µg L^{-1}) at Station BR44 where the total number of diatom cells per ml was also very low (<20 cells ml^{-1}). This was true also for Stations BR04 and BR09. The highest concentration of Chl-*a* was at Station BR81 (4.96 µg L^{-1}) and the lowest at Station BR50 (0.05 µg L^{-1}) (Figure 7). Chl-*a* concentrations rose steadily from Station BR41 to Station BR81 across the 60°S latitude. At the start and end of the 'buoy run' (at the stations closest to the ice), Chl-*a* concentrations were generally low (<0.5 µg L^{-1}), while at the midway stations (between the ice and South Georgia), Chl-*a* concentrations were generally higher (>1.0 µg L^{-1}). The station with the highest abundance of diatoms was Station BR89, with 5,622 cells ml^{-1}. By contrast, the station with the lowest number of diatoms was Station BR44 (sampled within the fjord at South Georgia), with just 18 cells ml^{-1}.

Of the more abundant, larger phytoplankton species, such as *Corethron* sp., *Dactyliosolen* sp., large (>30 µm) *Chaetoceros* sp. and large (>40 µm) *Fragilariopsis* sp., most were, on average, more abundant in the Weddell Sea than in the Scotia Sea. With the exception of Station BR44 (which occupies a different water mass), most stations sampled in the Scotia Sea were numerically dominated by small nanoplankton such as small F*ragilariopsis* sp. and *Chaetoceros* sp. (Figure 11a); however with respect to biomass (pg C l^{-1}), microplankton dominated (>50%) the community at almost all stations, with the exception of three stations close to the ice: BR01, BR03 and BR89 (Figure 11b). *Eucampia antarctica* occurred at only a few stations in low numbers, (BR1, BR3, BR46, BR52 and BR89), mostly in the Weddell Sea, where dSi generally exceeded concentrations found in the Scotia Sea, which is consistent with *Eucampia antarctica* having a high dSi demand (Poulton et

al., 2007a).

Lowest overall cell abundance occurred at South Georgia (Station BR44) – but, this was not an indication of low biomass, as the dominant species found at this station was *Corethron sp*., a very large species (~300 µm in length) with high dSi requirements (Poulton et al., 2007). This implies that if abundance was converted to cell carbon (for *Corethron* sp. cell carbon ranges between 3781 pg C l^{-1} and 8628 pg C l^{-1}, depending on the species), this site does exhibit a relatively high biomass (50.8 pg C l^{-1}) (Figure 11b), even though chlorophyll biomass was also at its lowest. This highlights the potential discrepancy and variability in cellular carbon to Chl-*a* ratios. Elsewhere, Chl-*a* concentrations increased exponentially across the Weddell and Scotia Sea boundary on the southward leg of the 'buoy run', which coincided with the first period of sun after weeks of windy, overcast days. Conversely, the highest overall cell abundance was recorded at Station BR89 at the end of the 'buoy run', with over 5000 cells ml^{-1} of seawater and a total biomass of 96.7 pg C l^{-1} a station sampled amongst the melting ice. Interestingly, nanoplankton were the dominant group in both biomass and numbers.

While small (<99 pg C cell^{-1}) and medium phytoplankton (100–999 pg C cell^{-1}) greatly outnumbered the larger phytoplankton species (defined as >1000 pg C cell^{-1}) (Hinz et al., 2012), in terms of cell numbers per ml, and in terms of cell carbon, pico- and nanoplankton groups dominated at only a few stations (BR01, BR03 and BR89). These stations were situated closest to the ice shelf, suggesting that the population had been seeded by sea-ice melt (Walker et al., 1986). Salinity at this station was low, 33.5, and Walker et al. (1986) suggested that the primary mechanism to explain ice edge blooms is low-salinity water from ice-melt, which produces a stable surface layer and a good light environment for growth. As mentioned previously, Sakshaug and Holm-Hansen (1986) proposed that blooms would only develop in shallow mixed layer depths of <40 m characterised by a favourable light environment, as was the case at Station BR89 (~30 m).

5 Conclusions

Mineralised nanoplanktonic size classes may be far more important than previously thought. This study shows it to be a far more important size class in this region at this time of year than expected. Indeed, mineralising phytoplankton specifically are an important component of the biological carbon pump, playing an important role in the draw-down of organic material from the surface to the deep sea (Francois et al., 2002; Buesseler and Boyd, 2009). This study shows the importance of not underestimating this size class and shows the value of using tools such as scanning electron microscopy to enumerate phytoplankton species. However it is important to note that this study focused specifically on mineralising nanoplankton and that due to the filters employed larger cells may have been underestimated. Thus employing the use of SEM in addition to traditional methods used to enumerate phytoplankton species.

The importance of SST in determining the distribution of phytoplankton groups is clear and with warming oceans, the effect of temperature on the smaller size classes of phytoplankton, especially on coccolithophores, needs to be recognized and further examined. Temperature is a particularly important factor in understanding the distribution of *E. huxleyi*, which appears to be moving further south in the Southern Ocean (Cubillos et al., 2007).

These results support and extend previous work done on the importance of diatoms in the Southern Ocean (Boyd, 2002), as well as the importance of the smaller size fractions (nano- and picoplankton). The clear distinction between the Scotia and Weddell Sea phytoplankton communities, with warmer, more salty, northern waters contrasting cooler, fresher, more southern waters, may enable us to better understand phytoplankton responses to possible ocean warming in the future. It is clear that the differentiation of phytoplankton communities is dependent on environmental gradients such as dSi and temperature (SST). With the threat of ocean warming in the future these results have important implications for predicting how future Southern Ocean phytoplankton communities will respond to change. Perhaps the distribution of coccolithophores like *E. huxleyi* will move further south as temperatures increase, as well as species like *Tetraparma pelagica*, which appears to be strongly associated with *E. huxleyi*. However, the southern advance of their distribution is also likely to be curtailed by calcite undersaturation.

To unravel these competing theories and conflicting evidence, further work is required, and it would be advisable to repeat this study in multiple years with an extended data set. Unfortunately, while iron data were collected during the cruise, it was not run because the flow injection analyser was not working properly (in fact is still not working properly) and therefore the iron values were unavailable for this thesis. Future studies should include iron, pCO_2 and irradiance measurements to obtain a more complete view of this oceanic region. Lastly, incubation bioassays where in situ conditions are modified, would also help to tease apart the different controls (e.g. iron vs. temperature vs. irradiance) on mineralising phytoplankton growth in the Southern Ocean.

References

1. Arrigo, K. R., Worthen, D., Schell, A., Lizotte, M. P. 1998. Primary production in Southern Ocean waters. *Journal of Geophysical Research*, **103**: 15587-15600.

2. Arrigo, K. R., Robinson, D. H., Worthen, D. L., Dunbar, R. B., Ditullio, G. R., VanWoert, M., Lizotte, M. P. 1999. Phytoplankton Community Structure and the Drawdown of Nutrients and CO_2 in the Southern Ocean. *Science*, **283**: 365-367.

3. Arrigo, K. R., Thomas, D. N. 2004. Large scale importance of sea ice biology in the Southern Ocean. *Antarctic Science*, **16**: 471-486.

4. Arrigo, K. R., van Dijken, G. L., Bushinsky, S. 2008. Primary production in the Southern Ocean, 1997 – 2006. *Journal of Geophysical Research*, **113**: C08004, doi:10.1029/2007JC004551.

5. Banse, K. 1996. Low seasonality of low concentrations of surface chlorophyll in the Subantarctic water ring: underwater irradiance, iron, or grazing? *Progress in Oceanography*, **37**: 241-291.

6. Bathmann, U. V., Scharek, R., Klaas, C., Dubischar, C. D., Smetacek, V. 1997. Spring development of phytoplankton biomass and composition in major water masses of the Atlantic sector of the Southern Ocean. *Deep-Sea Research II*, **44**: 51-67.

7. Blain, S., Sarthou, G., & Laan, P. 2008. Distribution of dissolved iron during the natural iron-fertilization experiment KEOPS (Kerguelen Plateau, Southern Ocean). *Deep-Sea Research II*, **55**: 594–605.

8. Boyd, P.W., Robinson, C., Savidge, G., Williams, P.J., Le, B., 1995. Water column and sea ice primary production during austral spring in the Bellingshausen Sea. *Deep-Sea Research II*, **42**: 1177–1200.

9. Boyd, P. W. 2002. Review: Environmental Factors Controlling Phytoplankton Processes in the Southern Ocean. *Journal of Phycology*, **38**: 844-861.

10. Buesseler, K. O., Boyd, P. W. 2009. Shedding light on processes that control particle export and flux attenuation in the twilight zone of the open ocean. *Limnology and Oceanography*, **54**: 1210-1232.

11. Clarke, K.R., Gorley, R.N. 2006. PRIMER v6: User Manual/Tutorial Plymouth, PRIMER-E.

12. Cochlan, W. P., Herndon, J., Kudela, R. M. 2008. Inorganic and organic nitrogen uptake by the toxigenic diatom *Pseudo-nitzschia australis* (*Bacillariophyceae*). *Harmful Algae*, 8: 111-118.

13. Cubillos, J. C., Wright, S. W., Nash, G., de Salas, M. F., Griffiths, B., Tilbrook, B., Poisson, A. & Hallegraeff G. M. 2007. Calcification morphotypes of the coccolithophorid *Emiliania huxleyi* in the Southern Ocean: changes in 2001 to 2006 compared to historical data. *Marine Ecology Progress Series*, **348**: 47–54.

14. Cullen, J. J. 1991. Hypotheses to explain High-Nutrient Conditions in the Open Sea. *Limnology and Oceanography*, **36**: 1578-1599.

15. Daly, K. L., Smith, W. O., Johnson, G. C., DiTuillo, G. R., Jones, D. R., Mordy, C. W., Feely, R. A., Hansell, D. A., Zhang, J.-Z. 2001. Hydrography, nutrients, and carbon pools in the Pacific sectors of the Southern Ocean: Implications for carbon flux. *Journal of Geophysical Research*, **106**: 7107–24.

16. de Baar, H. J. W., De Jong, J. T. M., Bakker, D. C. E., Löscher, B. M., Veth, C., Bathmann, U., Smetacket, V. Importance of iron for plankton blooms and carbon dioxide drawdown in the Southern Ocean. *Nature*, **373**: 412-415.

17. de Baar, H. J. W., Boyd, P. W., Landry, M. R., Tsuda, A., Assmy, P.,Bakker, D. C. E., Bozec, Y., Barber, R. T., Brzezinski, M. A., Buesseler, K. O., Boyé, M., Croot, P. L., Gervais, F., Gorbunov, M. Y., Harrison, P. J., Hiscock, W. T., Laan, P., Lancelot, C., Law, C. S., Levasseur, M., Marchetti, A., Milero, F. J., Nishioka, J., Nojiri, Y., van Oijen, T., Riebesell, U., Rijkenberg, M. J. A., Saito, H., Takeda, S., Timmermans, K. R., Veldhuis, M. J. W., Waite, A. M., Wong, C.-S. 2005. Synthesis of iron fertilization experiments: From the Iron Age in the Age of Enlightenment. *Journal of Geophysical Research*, **110**: [doi:10.1029/2004JC002601].

18. de Boyer Montégut, C., Mignot, J., Lazar, A. and Cravatte, S., 2007. Control of salinity on the mixed layer depth in the world ocean: 1. General description. *Journal of Geophysical Research*, **112**(C6): C06011.

19. Eynaud, F., Giraudeau, J., Pichon, J.-J. & Pudsey, C.J. 1999. Sea-surface distribution of coccolithophores, diatoms, silicofagellates and dinofagellates in the South Atlantic Ocean during the late austral summer 1995. *Deep-Sea Research I*, **46**: 451-482.

20. Falkowski, P.G., Barber, R.T., Smetacek, V., 1998. Biogeochemical controls and feedbacks on ocean primary production. *Science*, **281**: 200-206.

21. Franck, V. M., Brzezinski, M. A., Coale, K. H., Nelson, D. M. 2000. Iron and silicic acid concentrations regulate Si uptake north and south of the Polar Frontal Zone in the Pacific Sector of the Southern Ocean. *Deep Sea Research Part II: Tropical Studies in Oceanography*, **47**: 3315-3338.

22. Francois, R., Honjo, S., Krishfield, R., Manganini, S., 2002. Factors controlling the flux of organic carbon to the bathypelagic zone of the ocean. *Global Biogeochemical Cycles*, **16**: [doi: 10.1029/2001GB001722].

23. Fofonoff, N. P., Millard, R. C. 1983. Algorithms for computation of fundamental properties of seawater. *UNESCO Technical Papers in Marine Sciences*, No. **44**: 53pp.

24. Gomi, Y., Taniguchi, A., Fukuchi, M. 2007. Temporal and spatial variation of the phytoplankton assemblage in the eastern Indian sector of the Southern Ocean in summer 2001/2002. *Polar Biology*, **30**: 817-827.

25. Grasshoff, K., Kremling, K., Ehrhardt, M. 1983. Determination of urea (9.5). In: Methods of Seawater Analysis, 2nd Edition. Verlag Chemie, Weinheim, Germany. Pp 158 -162

26. Gravalosa, J. M., Flores, J-A., Sierro, F. J. & Gersonde, R. 2008. Sea surface distribution of coccolithophores in the eastern Pacific sector of the Southern Ocean (Bellingshausen and Amundsen Seas) during the late austral summer of 2001. *Marine Micropaleontology*, **69**: 16-25.

27. Grotti, M., Soggia, F., Ianni, C., Frache, R. 2005. Trace metals distributions in coastal sea ice of Terra Nova Bay, Ross Sea, Antarctica. *Antarctic Science*, **17**: 289-300.

28. Gruber, N., Gloor, M., Mikaloff Fletcher, S. E., Doney, S. C., Dutkiewicz, S. 2009. Oceanic sources, sinks, and transport of atmospheric CO_2. *Global Biogeochemical Cycles*, **23**: GB1005, doi:10.1029/2008GB003349.

29. Hinz, D. J., Poulton, A. J., Nielsdóttir, M. C., Steigenberger, S., Korb, R. E., Achterberg, E. P., Bibby, T. S. 2012. Comparative seasonal biogeography of mineralising nannoplankton in the Scotia Sea: *Emiliania huxleyi, Fragilariopsis spp*. and *Tetraparma pelagica. Deep-Sea Research II*, **59-60**: 57-66.

30. Holligan, P. M., Charalampopoulou, A. & Hutson, R. 2010. Seasonal Distributions of the coccolithophore, *Emiliania huxleyi*, and of particulate inorganic carbon in surface waters of the Scotia Sea. *Journal of Marine Systems*, **82**: 195-205.

31. Hutchins, D. A., Bruland, K. W. 1998. Iron-limited diatom growth and Si:N uptake ratios in a coastal upwelling regime. *Nature*, **393**: 561-564.

32. Kang, S.-H., Lee, S., Chung, K. H., Kim, D., Park, M. G. 2001. Antarctic phytoplankton assemblages in the marginal ice zone of the northwestern Weddell Sea. *Journal of Plankton Research*, **23**: 33–352.

33. Klaas, C., Archer, D.E., 2002. Association of sinking organic matter with various types of mineral ballast in the deep sea: implications for the rain ratio. *Global Biogeochemical Cycles*, **16**: [doi: 10.1029/2001GB001765].

34. Korb, R. E., Whitehouse, M. J., Ward, P. 2004. SeaWiFS in the Southern Ocean: spatial and temporal variability in phytoplankton biomass around South Georgia. *Deep Sea Research Part II*: Tropical Studies in Oceanography, 51: 99-116.

35. Korb, R. E., Whitehouse, M. J., Atkinson, A., Thorpe, S. 2008. Magnitude and maintenance of the phytoplankton bloom at South Georgia: a naturally iron-replete environment. *Marine Ecology Progress Series*, **368**: 75-91.

36. Korb, R. E., Whitehouse, M. J., Gordon, M., Ward, P., Poulton, A. J. 2010. Summer microplankton community structure across the Scotia Sea: implications for biological carbon export. *Biogeosciences*, **7**: 343-356.

37. Korb, R. E., Whitehouse, M. J., Ward, P., Gordon, M., Venables, H. J., Poulton, A. J. 2012. Regional and seasonal differences in microplankton biomass, productivity, and structure across the Scotia Sea: Implications for the export of biogenic carbon. *Deep-Sea Research II*, **59-60**: 67-77.

38. Lannuzel, D., Schoemann, V., de Jong, J., T, J-L., Chou, L. 2007. Distribution and biogeochemical behaviour of iron in the East Antarctic sea ice. *Marine Chemistry*, 106: 18-32.

39. Laubscher, R. K., Perissinotto, R., McQuaid, C. D. 1993. Phytoplankton production and biomass at frontal zones in the Atlantic sector of the Southern Ocean. *Polar Biology*, **13**: 471-481.

40. Levitus, S., Conkright, M. E., Reid, J. L., Najjar, R. G., Mantyla, A. 1993. Distribution of nitrate; phosphate and silicate in the world oceans. *Progress In Oceanography*, **31**: 245-273.

41. Levitus, S., 1982: Climatological Atlas of the World Ocean. NOAA Prof. Paper 13, 173 pp. and 17 microfiche.

42. Lucas, M., Seeyave, S., Sanders, R., Mark Moore, C. M., Williamson, R., & Stinchcombe, M. 2007. Nitrogen uptake responses to a naturally Fe-fertilised phytoplankton bloom during the 2004/2005 CROZEX study. *Deep-Sea Research II*, **54**: 2138–2173.

43. Maldonado, M. T., Boyd, P. W., Harrison, P. J., Price, N. M. 1999. Co-limitation of phytoplankton growth by light and Fe during winter in the NE subarctic Pacific Ocean. *Deep Sea Research Part II: Tropical Studies in Oceanography*, **46**: 2475-2485.

44. Martin, J. H. 1990. Glacial-interglacial CO_2 Change: The Iron Hypothesis. *Paleoceanography,* **5**: 1-13.

45. Mitchell, B. G., Brody, E. A., Holm-Hansen, O., McClain, C., Bishop, J. 1991. Light limitation of phytoplankton biomass and macronutrient utilization in the Southern Ocean. *Limnology and Oceanography*, **36**: 1662-1677.

46. Moore, G. F., Aiken, J., Lavender, S. J. 1999. The atmospheric correction of water colour and the quantitative retrieval of suspended particulate matter in Case II waters: Application to MERIS. *International Journal of Remote Sensing,* **20**: 1713-1733.

47. Moore, J. K., Abbott, M. R. 2002. Surface chlorophyll concentrations in relation to the Antarctic Polar Front: seasonal and spatial patterns from satellite observations. *Journal of Marine Systems*, **37**: 69-86.

48. Moore, J. K., & Scott C. Doney, S. C. 2007a. Iron availability limits the ocean nitrogen inventory stabilizing feedbacks between marine denitrification and nitrogen fixation. *Global Biogeochemical Cycles*, **21**: [doi:10.1029/2006GB002762]

49. Moore, C. M., Hickman, A. E., Poulton, A. J., Seeyave, S., & Lucas, M. I. 2007b. Iron–light interactions during the CROZet natural iron bloom and EXport experiment (CROZEX): II—Taxonomic responses and elemental stoichiometry. *Deep-Sea Research II,* **54**: 2066–2084.

50. Morel, F. M. M., Rueter, J. G., Price, N. M. 1991. Iron nutrition of phytoplankton and its possible importance in the ecology of ocean regions with high nutrients and low biomass. *Oceanography*, **4**: 56-61.

51. Murphy, E. J. 1995. Spatial structure of the Southern Ocean ecosystem: predator-prey linkages in Southern Ocean food webs. *Journal of Animal Ecology*, **64**: 333-347.

52. Nelson, D. M., Smith, W. O. 1991. Sverdup revisited: Critical depths, maximum chlorphyll levels, and the control of the Southern Ocean productivity by the irradiane-mixing regime. *Limnology and Oceanography*, **36**: 1650-1661.

53. Nielsdottir, M C., Bibby, T. S., Moore, C. M., Hinz, D. J., Sanders, R., Whitehouse, M., Korb, R., Achterberg, E. P. 2012. Seasonal and spatial dynamics of iron availability in the Scotia Sea. *Marine Chemistry*, **130-131**: 62-72.

54. Orsi, A. H., Whitworth III, T., Nowlin Jr, W. D. 1995. On the meridional extent and fronts of the Antarctic Circumpolar Current. *Deep-Sea Research I*, **42**: 641-673.

55. Parsons, T. R., Maita, Y., Lalli, C. M. 1984. Plant Pigments. Pergamon Press, 173pp.

56. Pollard, R. T., Salter, I., Sanders, R. J., Lucas, M. I., Moore, C. M., Mills, R. A., Statham, P. J., Allen, J. T., Baker, A. R., Bakker, D. C. E., Charette, M. A., Fielding, S., Fones, G. R., French, M., Hickman, A. E., Holland, R. J., Hughes, J. A., Jickells, T. D., Lampitt, R. S., Morris, P. J., Nédélec, F. H., Nielsdóttir, M., Planquette, H., Popova, E. E., Poulton, A. J., Read, J. F., Seeyave, S., Smith, T., Stinchcombe, M., Taylor, S., Thomalla, S., Venables, H. J., Williamson, R., & Zubkov, M. V. 2009. Southern Ocean deep-water carbon export enhanced by natural iron fertilization. *Nature*, **457**: 577-580.

57. Poulton, A. J., Moore, M., Seeyave, S., Lucas, M. I., Fielding, S. & Ward, P. 2007a. Phytoplankton community composition around the Crozet Plateau, with emphasis on diatoms and Phaeocystis. *Deep-Sea Research II*, **54**: 2085–2105.

58. Poulton, A.J., Adey, T.R., Balch, W.M., Holligan, P.M. 2007b. Relating coccolithophore calcification rates of phytoplankton community dynamics: Regional differences and implications for carbon export. *Deep-Sea Research II*, **54**: 538-557.

59. Raven, J. A. 1990. Predictions of Mn and Fe use efficiencies of phototrophic growth as a function of light availability for growth and for C assimilation pathways. *New Phytologist*, **116**(1): 1-18.

60. Rintoul, S. R., and J. L. Bullister, 1999: A late winter hydrographic section from Tasmania to Antarctica. *Deep-Sea Research I*, **46**: 1417–1454.

61. Sabine, C. L., Feely, R. A., Gruber, N., Key, R. M., Lee, K., Bullister, J. L., Wanninkhof, R., Wong, C. S., Wallace, D. W. R., Tilbrook, B., Millero, F. J., Peng, T-H., Kozyr, A., Ono, T., Rios, A. F. 2004. The Oceanic Sink for Anthopogenic CO_2. *Science*, **305**: 367-371.

62. Sakshaug, E., Holm-Hansen, O. 1986. Photoadaptation in Antarctic phytoplankton variations in growth rate, chemical composition and P versus I curves. *Journal of Plankton Research*, **8**: 459-473.

63. Scott, F.J., Marchant, H.J., 2005. Antarctic Marine Protists. Australian Biological Resources Study, Canberra.

64. Sedwick, P. N., DiTullio, G. R. 1997. Regulation of algal blooms in Antarctic Shelf Waters by the release of iron from melting sea ice. *Geophysical Research Letters,* **24**: 2515-2518.

65. Seeyave, S., Lucas, M.I., Moore, C.M., Poulton, A.J., 2007. Phytoplankton productivity and community structure in the vicinity of the Crozet Plateau during austral summer 2004/2005. *Deep-Sea Research II*, **54**: 2020-2044.

66. Smetacek, V., Klaas. C., Menden-Deuer, S., Rynearson, T. A. 2002. Mesoscale distribution of dominant diatom species relative to the hydrographical field along the Antarctic Polar Front. *Deep-Sea Research II*, **49**: 3835–3848.

67. Smetacek, V., Assmy, P., Henjes, J. 2004. The role of grazing in structuring Southern Ocean pelagic ecosystems and biogeochemical cycles. *Antarctic Science*, **16**: 541-558.

68. Smith, W. O., Lancelot, C. 2004. Bottom-up versus to-down control in phytoplankton of the Southern Ocean. *Antarctic Science*, **16**: 531-539.

69. Sokolov, S. Rintoul, S. R. 2002. Structure of Southern Ocean fronts at 140°E. *Journal of Marine Systems*, **37**: 151-184.

70. Sullivan, C. W., Arrigo, K. R., McClain, C. R., Comiso, J. C. & Firestone, J. 1993. Distributions of Phytoplankton Blooms in the Southern Ocean. *Science*, 262: 1832-1837.

71. Sunda, W. G., Huntsman, S. A. 1997. Interrelated influence of iron, light and cell size on marine phytoplankton growth. *Nature*. **390**: 389-392.

72. Takahashi, T., Sutherland, S. C., Wanninkhof, R., Sweeney, C., Feely, R. A., Chipman, D. W., Hales, B., Friederich, G., Chavez, F., Sabine, C., Watson, A., Bakker, D. C. E., Schuster, U., Metzl, N., Yoshikawa-Inoue, H., Ishii, M., Midorikawa, T., Nojiri, Y., Körtzinger, A., Steinhoff, T., Hoppema, M., Olafsson, J., Arnarson, T. S., Tilbrook, B., Johannessn, T., Olsen, A., Bellerby, R., Wong, C. S., Delille, B., Bates, N. R., de Baar, H. J. W. 2009. Climatological mean and decadal change in surface ocean pCO_2, and net sea-air CO_2 flux over the global oceans. *Deep Sea Reseach Part II: Tropical Studies in Oceanography*, **56**: 554-577.

73. Takeda, S. 1998. Influence of iron availability on nutrient consumption ratio of diatoms in oceanic waters. *Nature*, 393: 774-777.

74. Thomalla, S. J., Poulton, A. J., Sanders, R., Turnewitsch, R., Holligan, P. M. & Lucas, M. I. 2008. Variable export fluxes and efficiencies for calcite, opal and organic carbon in the Atlantic Ocean: A ballast effect in action? *Global Biogeochemical Cycles*, **22**: [doi:10.1029/2007GB002982].

75. Tomas, C. R. 1997. Identifying Marine Plankton. Academic Press.

76. Van Franeker, J. A., van den Brink, N. W., Bathmann, U. V., Pollard, R. T., de Baar, H. J. W., Wolff, W. J. 2002. Responses of seabirds, in particular prions (Pachyptila sp.), to small-scale processes in the Antarctic Polar Front. *Deep-Sea Research II*, **49**: 3931–3950.

77. Walker, O., Smith, Jr., Nelson, D. M. 1986. Importance of Ice Edge Phytoplankton Production in the Southern Ocean. *Biological Sciences*, **36**: 251-257.

78. Ward, P., Whitehouse, M., Meredith, M., Murphy, e., Shreeve, R., Korb, R., Watkins, J., Thorpe, S., Woodd-Walker, R., Brierley, A., Cunningham, N., Grant, S., Bone, D. 2002. The Southern Antarctic Circumpolar Current Front: physical and biological coupling at South Georgia. *Deep-Sea Research I*, **49**: 2183-2202.

79. Ward, P., Atkinson, A., Tarling, G. 2012. Mezozooplankton community structure and variability in the Scotia Sea: A Seasonal Comparison. *Deep-Sea Research II*, **59**: 78-92.

80. Whitehouse, M. J., Atkinson, A. Korb, R. E., Venables, H. J., Pond, D. W., Gordon, M. 2012. Substantial primary production in the land-remote region of the central and northern Scotia Sea, *Deep-Sea Research II*, **59**: 47-96.

81. Winter, A., Elbrächter, M. & Krause, G. 1998. Subtropical coccolithophores in the Weddell Sea. *Deep-Sea Research I*, **46**: 439-449.

82. Wright, S. W., van den Enden, R. L. 2000. Phytoplankton community structure and stocks in the East Antarctic marginal ice zone (BROKE survey, January – March 1996) determined by CHEMTAX analysis of HPLC pigment signatures. *Deep Sea Research Part II: Tropical Studies in Oceanography*, **47**: 2363-2400.

83. Wright, S. W., van den Enden, R. L., Pearce, I., Davidson, A. T., Scott, F. J., Westwood, K. J. 2010. Phytoplankton community structure and stocks in the Southern Ocean (30-80°E) determined by CHEMTAX analysis of HPLC pigment signatures. *Deep Sea Research Part II: Tropical Studies in Oceanography*, **57**: 758-778.

84. Zentara, S. J. and Kamykowski, D. 1981. Geographic variations in the relationship between silicic acid and nitrate in the South Pacific Ocean. *Deep Sea Research Part A. Oceanographic Research Papers,* **28**: 455-465.

85. Ziveri, P., de Bernardi, B., Baumann, K.H, Stoll, H. M., Mortyn, P. G. 2007. Sinking of coccolith carbonate and potential contribution to organic carbon ballasting in the deep ocean. *Deep-Sea Research II,* **54**: 659-675.

Appendices

Appendix A: Hydrographic data

Date	Station No.	Latitude	Longitude	Time	SST	Salinity	MLD	NO_3^-	$SiOH_4^{4-}$
					(°C)		(m)	($\mu g L^{-1}$)	($\mu g L^{-1}$)
16/01/10	BR01	-69.8939	-1.7484	22:05:00	1.876	33.39	13.5	11.146	42.79
17/01/10	BR03	-69.3267	-1.8345	06:05:00	1.026	33.37	13.5	21.217	20.94
17/01/10	BR04	-69.0383	-1.7033	09:00:00	2.619	34.07	13.5	23.151	48.98
17/01/10	BR05	-68.2603	-2.6978	14:10:00	2.591	34.04	23	24.877	36.29
17/01/10	BR06	-67.6064	-3.5581	18:06:00	2.341	33.97	33	24.906	42.76
17/01/10	BR07	-67.139	-4.1068	21:04:00	2.197	33.84	24.5	24.993	50.07
18/01/10	BR08	-66.439	-5.0374	01:58:00	2.028	33.88	24.5	22.784	48.48
18/01/10	BR13	-63.6257	-8.274	21:25:00	0.587	33.34	15.5	20.486	missing
19/01/10	BR19	-61.651	-12.9743	21:13:00	1.793	34.16	27	18.355	34.52
20/01/10	BR25	-60.639	-20.9597	20:58:00	3.26	34.11	50.5	18.904	33.19
21/01/10	BR31	-59.2015	-28.3573	21:00:00	2.828	34.21	19.5	23.94	missing
22/01/10	BR37	-56.3728	-33.2687	21:00:00	3.698	33.93	19	20.567	19.43
24/01/10	BR44	-54.1388	-36.4065	06:13:00	4.254	33.44	13	21.717	10.67
25/01/10	BR46	-53.276	-33.805	09:07:00	4.368	33.95	25.5	22.036	8.99
26/01/10	BR52	-54.3439	-27.4993	09:04:00	3.884	34.08	35	21.61	missing
27/01/10	BR58	-57.4533	-23.0668	08:59:00	3.975	34.06	41	20.377	27.43
27/01/10	BR61	-58.9393	-20.285	21:04:00	3.072	34.01	28.5	21.354	32.91
30/01/10	BR79	-63.5242	-5.0483	21:09:00	2.248	33.68	22	16.578	47.8
31/01/10	BR81	-65.1043	-5.1064	06:01:00	2.249	33.7	29	17.473	35.31
31/01/10	BR82	-65.5927	-4.9938	09:00:00	2.25	33.68	24.5	18.442	42.67
31/01/10	BR85	-67.6093	-5.0467	21:05:00	2.12	33.86	39	22.733	missing
01/02/10	BR86	-68.3782	-5.5163	02:10:00	2.244	34.06	45	25.486	43.13
01/02/10	BR87	-69.0517	-6.2499	06:00:00	2.08	34.12	36	24.881	49.6
01/02/10	BR88	-69.49	-7.0102	09:37:00	1.855	33.96	36	25.155	41.79
01/02/10	BR89	-70.0415	-7.9263	14:39:00	1.206	33.46	36	22.645	43.46

Appendix B:List of species found at each station

Species	BR01	BR03	BR04	BR05	BR06	BR07	BR08	BR13	BR19	BR25	BR31	BR37	BR44	BR46	BR52	BR58	BR61	BR79	BR81	BR82	BR85	BR86	BR87	BR88	BR89
Asteromphalus sp.	1.61	2.83	0.46	0.00	0.00	0.91	1.29	5.44	0.00	2.06	0.45	0.00	0.00	0.45	0.46	2.79	1.37	18.65	16.00	19.25	2.30	0.46	1.84	0.91	1.37
Large *Chaetoceros* sp.	2.54	3.40	0.46	0.46	2.30	2.27	0.00	7.42	13.63	2.58	0.00	1.37	0.00	5.46	1.85	0.00	0.00	28.69	23.10	1.48	4.13	4.17	1.84	0.91	0.00
Medium *Chaetoceros* sp.	14.29	7.37	18.44	11.02	11.02	6.37	3.22	129.57	185.21	11.35	8.64	52.10	2.65	150.14	69.94	93.06	5.03	153.49	145.73	26.65	85.38	31.50	24.33	17.82	8.68
Small *Chaetoceros* sp.	18.68	56.67	100.98	39.48	28.46	30.48	30.90	306.61	97.01	238.81	48.23	132.07	5.29	1225.23	542.41	293.14	72.66	97.55	263.03	88.85	179.95	52.81	126.24	38.39	63.98
Large *Corethron* sp.	0.00	0.00	0.92	4.59	1.84	2.27	0.64	1.48	0.80	0.00	0.00	0.46	5.82	0.45	1.39	3.72	0.00	0.00	0.00	5.92	1.38	7.87	1.38	2.29	0.91
Small *Corethron* sp.	0.00	0.00	2.31	9.64	7.34	5.00	1.29	10.88	19.24	1.03	0.00	1.37	0.00	1.36	8.34	4.65	0.46	12.91	44.43	7.40	8.72	31.50	2.75	5.48	0.46
Cylindrotheca sp.	0.46	0.57	65.02	0.00	2.75	26.39	19.95	58.85	66.55	28.88	385.36	14.17	0.00	4.09	4.63	3.72	40.22	117.63	611.36	102.18	43.61	95.88	124.40	73.58	166.81
Dactyliosolen sp.	0.46	0.00	10.14	0.00	5.05	0.45	3.86	3.96	8.82	45.39	0.00	0.00	0.00	0.00	6.95	0.93	0.00	4.30	1.78	0.00	0.00	0.00	0.00	0.00	0.00
Dictyocha sp.	16.60	21.54	0.46	1.84	0.00	0.00	1.93	21.76	1.60	9.80	0.00	0.00	0.00	1.82	9.73	2.79	0.91	7.17	10.66	23.69	11.02	102.37	0.46	5.94	3.66
Emiliania huxleyi	0.00	0.00	0.00	0.00	0.00	0.00	0.00	0.00	0.00	138.23	0.00	8.68	0.00	4.09	8.34	266.16	57.58	0.00	0.00	0.00	0.00	0.00	0.00	0.00	0.00
Eucampia sp.	1.84	0.57	0.00	0.00	0.00	0.00	0.00	0.00	0.00	0.00	0.00	0.00	0.00	2.27	1.39	0.93	0.46	0.00	0.00	0.00	0.00	0.00	1.84	0.00	4.11
Large *Fragilariopsis* sp.	31.36	40.24	5.07	0.00	2.75	3.18	6.44	3.96	7.22	1.03	1.36	0.00	0.00	2.27	2.78	6.51	0.46	4.30	55.09	19.25	3.67	0.46	0.46	9.60	11.88
Medium *Fragilariopsis* sp.	146.64	457.35	29.97	40.86	72.99	37.76	46.34	93.96	179.59	25.27	41.86	6.86	0.53	11.37	14.82	25.13	6.86	77.46	318.12	186.58	39.02	43.08	78.96	38.39	508.64
Medium *Fragilariopsis* sp.	921.08	1151.59	141.10	1852.72	921.77	1349.44	305.10	397.11	521.14	617.40	1037.33	1169.46	2.12	54.60	83.84	98.65	1507.19	1121.80	1905.18	691.54	591.71	1394.71	2647.34	2415.25	4666.89
Haslea sp.	1.15	3.97	20.75	6.89	1.38	3.64	2.57	0.00	0.00	5.16	5.46	4.57	0.00	3.64	6.95	4.65	0.91	7.17	7.11	5.92	7.34	8.34	11.48	9.60	13.25
Leptocylindrus mediterraneus	0.00	0.00	0.00	0.00	0.00	0.00	0.00	0.00	0.00	1.55	0.00	0.00	0.00	0.00	3.24	0.93	0.00	0.00	0.00	0.00	0.00	0.00	0.00	0.00	0.00
Nitzschia sp.	41.50	37.40	8.30	97.32	24.33	24.57	21.24	46.49	57.73	82.01	120.11	3.66	0.00	3.64	7.41	1.86	19.19	114.76	129.74	96.25	8.26	42.15	106.04	42.96	107.40
Proboscia sp.	0.23	1.13	2.77	0.00	1.84	0.00	0.64	0.99	0.00	4.13	10.01	0.00	0.00	1.82	10.65	0.00	0.46	21.52	3.55	0.00	0.92	0.00	0.00	0.46	0.00
Prorocentrum sp.	0.00	0.00	0.00	0.00	0.00	0.00	0.00	0.00	0.00	0.00	0.00	2.74	0.00	1.82	0.00	40.95	0.00	0.00	0.00	0.00	0.00	0.00	0.00	0.00	0.00
Pseudonitzschia sp.	0.46	4.53	3.23	3.21	4.13	2.27	1.29	17.80	1.60	34.56	8.64	4.11	0.00	72.80	150.08	204.74	7.77	180.75	120.85	19.25	16.53	1.85	12.39	12.34	24.22
Rhizosolenia sp.	0.23	1.13	19.37	0.00	14.23	16.38	0.64	4.45	8.82	12.38	13.19	0.00	0.00	9.55	28.26	3.72	134.36	51.64	47.99	11.85	28.00	5.10	0.46	29.71	0.00
Scripsiella troichoidea	0.46	0.00	0.00	0.00	0.00	0.91	0.64	0.00	0.00	0.00	0.00	0.00	0.00	0.00	0.00	0.00	0.00	0.00	0.00	0.00	0.00	0.00	0.92	0.46	0.00
Thallossisiosira sp.	0.00	0.00	0.00	0.00	0.00	0.45	0.00	0.00	0.00	30.43	5.46	0.91	1.06	1.36	0.46	26.06	46.61	0.00	0.00	0.00	1.38	0.93	9.18	5.94	43.87
Tetraparma pelagica sp.	0.00	0.57	0.00	5.51	1.38	16.83	5.79	0.99	0.00	485.87	116.93	15.08	0.00	1.36	12.51	1180.02	790.61	2.87	5.33	1.48	1.84	0.93	12.39	6.40	5.48